Table 3. Genes up-regulated in $CD4^+$ T cells from cord blood samples 1 and 2 (CB 1 and CB 2, respectively)

		Fold change				
Affi ID	Gene abbreviation	CB 1	CB 2	PB 1	PB 2	Gene name
Apoptosis						
1555372_at	*BimL*	1·39	1·52	0·61	0·42	BCL2-like 11 (apoptosis facilitator)
237837_at	*BCL2*	1·27	1·32	0·49	0·73	B-cell CLL/lymphoma 2
205681_at	*BCL2A1*	1·91	1·53	0·39	0·47	BCL2-related protein A1
1558143_a_at	*BCL2L11*	1·68	1·74	0·32	0·32	BGL2-like 11 (apoptosis facilitator)
228311_at	*BCL6B*	1·36	3·39	0·64	0·26	B-cell CLL/lymphoma 6, member B (zinc finger protein)
215037_s_at	*BCLX*	2·56	1·27	0·73	0·56	BCL2-like 1
224414_s_at	*CARD6*	2·65	1·34	0·56	0·66	Caspase recruitment domain family, member 6
201631_s_at	*IER3*	1·62	2·95	0·38	0·31	Immediate early response 3
218000_s_at	*PHLDA1*	2·34	1·21	0·53	0·79	Pleckstrin homology-like domain, family A, member 1
209803_s_at	*PHLDA2*	2·87	1·32	0·31	0·68	Pleckstrin homology-like domain, family A. member 2
203063_at	*PPMIF*	1·26	1·53	0·74	0·64	Protein phosphatase IF (PP2C domain containing)
205214_at	*STK17B*	1·78	1·26	0·74	0·71	Serine/threonine kinase 17b (apoptosis-inducing)
217853_at	*TENS1*	1·63	6·00	0·04	0·37	Tensin 1
B- and T-cell development						
211861_x_at	*CD28*	1·35	1·41	0·49	0·65	CD28 antigen(Tp44)
207892_at	*CD40LG*	3·67	1·32	0·45	0·68	C040 ligand (TNF superfamily, member 5, hyper-IgM syndrome)
206914_at	*CRTAM*	2·76	1·60	0·40	0·36	Class I MHC-restricted T-cell-associated molecule
210557_x_at	*CSF1*	3·79	1·22	0·78	0·70	Colony-stimulating factor 1 (macrophage)
210229_s_at	*CSF2*	1·28	2·67	0·69	0·72	Colony-stimulating factor 2 (granulocyte–macrophage)
205159_at	*CSF2RB*	2·33	1·60	0·18	0·40	Colony-stimulating factor 2 receptor
231794_at	*CTLA4*	1·39	1·26	0·74	0·44	Cytotoxic T-lymphocyte-associated protein 4
204232_at	*FCER1G*	1·63	2·14	0·28	0·37	Fc fragment of IgE, high affinity 1, receptor for; gamma polypeptide
210439_at	*ICOS*	1·38	1·34	0·57	0·66	Inducible T-cell costimulator
210354_at	*IFNG*	1·48	1·92	0·46	0·52	Human mRNA for HuIFN -gamma interferon
230536_at	*PBX4*	1·48	1·26	0·50	0·74	Pre-B-cell leukaemia transcription factor 4
215540_at	*TCRA*	1·25	1·87	0·67	0·75	T-cell antigen receptor alpha
234440_al	*TCRD*	7·51	1·48	0·50	0·52	Human T-cell receptor delta-chain
Cell growth and maintenance						
213497_at	*ABTB2*	2·06	1·34	0·66	0·63	Ankyrin repeat and BTB (POZ) domain containing 2
201236_s_at	*BTG2*	1·60	1·23	0·60	0·77	BTG family, member 2
235287_at	*CDK6*	1·50	1·32	0·44	0·68	Cyclin-dependent kinase 6
209644_x_at	*CDKN2A*	2·90	1·21	0·67	0·79	Cyclin-dependent kinase inhibitor 2A (melanoma, p16, inhibits CDK4)
236313_at	*CDKN2B*	3·24	1·28	0·58	0·72	Cyclin-dependent kinase inhibitor 2B (p15, inhibits CDK4)
241984_at	*CHES1*	1·38	1·34	0·66	0·63	Checkpoint suppressor 1
202552_s_at	CRIM1	1·94	1·39	0·32	0·61	Cysteine-rich transmembrane BMP regulator 1 (chordin-like)
204844_at	*ENPEP*	1·64	1·75	0·09	0·36	Glutamyl aminopeptidase (aminopeptidase A)
205418_at	*FES*	1·39	1·80	0·61	0·25	Feline sarcoma oncogene
228572_at	*GRB2*	4·69	1·21	0·79	0·78	Growth factor receptor-bound protein 2
207688_s_at	*INHBC*	1·46	1·25	0·51	0·75	Inhibin, beta C
209744_x_at	*ITCH*	1·30	1·47	0·63	0·70	Itchy homolog E3 ubiquitin protein ligase (mouse)
201548_s_at	*JARID1B*	1·27	1·92	0·73	0·46	Jumonji, AT-rich interactive domain IB (RBP2-like)
203297_s_at	*JARID2*	1·42	1·28	0·54	0·72	Jumonji, AT-rich interactive domain 2
41387_r_at	*JMJD3*	1·82	1·24	0·76	0·65	Jumonji domain containing 3
205569_at	*LAMP3*	2·32	1·24	0·76	0·50	Lysosomal-associated membrane protein 3
214039_s_at	*LAPTM4B*	1·41	1·49	0·49	0·59	Lysosomal-associated protein transmembrane 4 beta
205857_x_at	*MSH3*	1·79	1·28	0·58	0·72	MutS homolog 3 (*E. coli*)
209550_at	*NDN*	3·42	1·38	0·17	0·62	Necdin homolog (mouse)
207943_x_at	*PLAGL1*	1·37	1·43	0·57	0·63	Pleiomorphic adenoma gene-like 1
204748_at	*PTGS2*	1·65	1·78	0·14	0·35	Prostaglandin-endoperoxide synthase 2
201482_at	*QSCN6*	1·32	1·23	0·38	0·77	Quiescin Q6
203743_s_at	*TDG*	1·47	1·23	0·54	0·77	Thymine-DNA glycosylase
204227_s_at	*TK2*	2·12	1·26	0·56	0·74	Thymidine kinase 2, mitochondrial

Table 3. Continued

Affi ID	Gene abbreviation	Fold change CB 1	CB 2	PB 1	PB 2	Gene name
Cytokines and chemokines						
207533_at	*CCL1*	1·67	1·48	0·52	0·49	Chemokine (C-C motif) ligand 1
205099_s_at	*CCR1*	4·70	1·21	0·61	0·79	Chemokine (C-C motif) receptor 1
207681_at	*CXCR3*	1·51	1·33	0·41	0·67	Chemokine (C-X-C motif) receptor 3
211469_s_at	*CXCR6*	1·58	1·95	0·32	0·42	Chemokine (C-X-C motif) receptor 6
206613_at	*IL-18R1*	2·32	1·38	0·61	0·62	Interleukin-18 receptor 1
207072_at	*IL-18RAP*	2·16	1·44	0·46	0·56	Interleukin-18 receptor accessory protein
212657_s_at	*IL-1RN*	1·44	3·12	0·56	0·37	Interleukin 1 receptor
206341_at	*IL-2RA*	1·52	1·27	0·73	0·66	Interleukin-2 receptor alpha
202859_x_at	*IL-8*	1·31	3·75	0·38	0·69	Interleukin-8
202643_s_at	*TNFAIP3*	1·61	1·25	0·67	0·75	Tumour necrosis factor, alpha-induced protein 3
202687_s_at	*TNFSF10*	2·83	1·23	0·67	0·77	Tumour necrosis factor (ligand) superfamily member 10
205599_at	*TRAF1*	2·25	1·32	0·68	0·61	Tumour necrosis factor receptor-associated factor 1
202871_at	*TRAF4*	1·43	1·58	0·57	0·48	Tumour necrosis factor receptor-associated factor 4
206366_x_at	*XCL1*	1·24	2·66	0·46	0·76	Chemokine (C motif) ligand 1
Signal transduction						
210538_s_at	*AIP1*	1·35	1·54	0·65	0·61	Baculoviral IAP repeat-containing 3
209369_at	*ANXA3*	1·39	6·82	0·61	0·05	Annexin A3
1554343_a_at	*BRDG1*	1·45	1·67	0·52	0·55	BCR downstream signalling 1
225946_at	*C12orf2*	3·20	1·77	0·23	0·23	Ras association (RaIGDS/AF-6) domain family 8
204392_at	*CAMK1*	1·26	1·62	0·74	0·54	Calcium/calmodulin-dependent protein kinase I
231042_s_at	*CAMK2D*	1·31	1·63	0·25	0·69	Calcium/calmodulin-dependent protein kinase (CaM kinase) II delta
205692_s_at	*CD38*	1·37	1·29	0·71	0·48	CD38 antigen (p45)
231747_at	*CYSLTR1*	3·16	1·45	0·55	0·43	Cysteinyl leukotriene receptor 1
211272_s_at	*DGKA*	1·43	1·23	0·77	0·54	Diacylglycerol kinase alpha 80 kDa
200762_at	*DPYSL2*	1·35	1·40	0·37	0·65	Dihydropyrimtdinase-like 2
208370_s_at	*DSCR1*	1·23	1·90	0·63	0·77	Down syndrome critical region gene 1
204794_at	*DUSP2*	1·55	2·57	0·39	0·45	Dual specificity phosphatase 2
204015_s_at	*DUSP4*	1·35	2·66	0·65	0·39	Dual specificity phosphatase 4
211333_s_at	*FASLG*	1·20	1·37	0·49	0·80	Fas ligand (TNF superfamily, member 6)
211535_s_at	*FGFR1*	1·23	2·79	0·70	0·77	Fibroblast growth factor receptor 1
224148_at	*FYB*	1·50	1·21	0·45	0·79	FYN binding protein (FYB-120/130)
209304_x_at	*GADD45B*	1·55	1·29	0·65	0·71	Growth arrest and DNA-damage-inducible beta
234284_at	*GNG8*	1·50	3·16	0·50	0·35	Guanine nucleotide binding protein (G protein), gamma 8
224285_at	*GPR174*	1·91	1·42	0·56	0·58	G protein-coupled receptor 174
223767_at	*GPR84*	4·41	1·44	0·05	0·56	G protein-coupled receptor 84
211555_s_at	*GUCY1B3*	1·66	1·73	0·34	0·03	Guanylate cyclase 1, soluble, beta 3
38037_at	*HBEGF*	1·54	1·36	0·55	0·64	Heparin-binding EGF-like growth factor
203820_s_at	*IMP-3*	1·83	2·18	0·17	0·17	IGF-II-mRNA-binding protein 3
203006_at	*INPP5A*	1·40	1·86	0·60	0·52	Inositol polyphosphate-5-phosphatase, 40 kDa
231779_at	*IRAK2*	1·93	1·46	0·46	0·54	Interleukin-1 receptor associated kinase 2
32137_at	*JAG2*	1·58	1·29	0·71	0·64	Jagged 2
203904_x_at	*KAI1*	1·65	1·59	0·41	0·25	CD82 antigen
235252_at	*KSR*	1·72	1·56	0·43	0·44	Kinase suppressor of ras 1
210948_s_at	*LEF1*	1·21	1·64	0·41	0·79	Hypothetical protein LOC641518
203236_s_at	*LGALS9*	1·48	1·27	0·73	0·51	Lectin, galactoside-binding, soluble, 9 (galectin 9)
220253_s_at	*LRP12*	1·27	1·30	0·31	0·73	Low-density lipoprotein-related protein 12
206637_at	*P2RY14*	1·32	1·48	0·39	0·68	Purinergic receptor P2Y, G-protein coupled, 14
210837_s_at	*PDE4D*	1·35	1·31	0·62	0·69	Phosphodiesterase 4D, cAMP-specific
206726_at	*PGDS*	6·45	1·40	0·60	0·43	Prostaglandin D2 synthase, haematopoietic
210617_at	*PHEX*	1·53	4·08	0·21	0·47	Phosphate regulating endopeptidase homologue, X-linked
206370_at	*PIK3CG*	1·23	1·32	0·50	0·77	Phosphoinositide-3-kinase, catalytic, gamma polypeptide
205632_s_at	*PIP5K1B*	1·32	1·42	0·64	0·68	Phosphalidylinositol-4-phosphate 5-kinase, type 1 beta

Table 3. Continued

Affi ID	Gene abbreviation	Fold change CB 1	CB 2	PB 1	PB 2	Gene name
215195_at	*PRKCA*	2·17	1·36	0·64	0·61	Protein kinase C, alpha
210832_x_at	*PTGER3*	4·44	1·47	0·07	0·53	Prostaglandin E receptor 3 (subtype EP3)
1553535_a_at	*RANGAP1*	1·58	1·39	0·58	0·61	Ran GTPase activating protein 1
234344_at	*RAP2C*	1·75	1·26	0·46	0·74	RAP2C, member of RAS oncogene family
223809_at	*RGS18*	2·12	1·67	0·15	0·33	Regulator of G-protein signalling 18
209882_at	*RIT1*	1·74	1·32	0·63	0·68	Ras-like without CAAX 1
209451_at	*TANK*	1·34	1·20	0·42	0·80	TRAF family member-associated NFKB activator
204924_at	*TLR2*	1·60	2·52	0·36	0·40	Toll-like receptor 2
217979_at	*TM4SF13*	1·21	2·47	0·30	0·79	Tetraspanin 13
209263_x_at	*TM4SF7*	2·05	1·41	0·58	0·59	Tetraspanin 4
Transcription						
1566989_at	*ARID1B*	1·42	1·27	0·09	0·73	AT-rich interactive domain 1B (SWIl-like)
203973_s_at	*CEBPD*	3·06	1·51	0·33	0·49	CCAAT/enhancer binding protein (C/EBP), delta
221598_s_at	*CRSP8*	1·60	1·29	0·71	0·68	Cofactor required for Spl transcriptional activation, subunit 8, 34 kDa
205249_at	*EGR2*	1·33	4·27	0·67	0·60	Early growth response 2 (Krox-20 homologue, *Drosophila*)
206115_at	*EGR3*	1·31	6·15	0·69	0·48	Early growth response 3
201328_at	*ETS2*	1·57	1·72	0·43	0·40	V-ets erythroblastosis virus E26 oncogene homologue 2 (avian)
218810_at	*FLJ23231*	2·13	1·37	0·63	0·63	Zinc finger CCCH-type containing 12A
209189_at	*FOS*	21·56	1·31	0·13	0·69	V-fos FBJ murine osteosarcoma viral oncogene homologue
223408_s_at	*FOXK2*	2·26	1·22	0·48	0·78	Forkhead box K2
202723_s_at	*FOXO1A*	1·47	1·27	0·57	0·73	Forkhead box O1A (rhabdomyosarcoma)
224211_at	*FOXP3*	1·62	1·41	0·59	0·23	Forkhead box P3
207156_at	*HIST1H2AG*	1·73	1·30	0·41	0·70	Histone 1, H2ag
220042_x_at	*HIVEP3*	1·26	1·65	0·74	0·56	Human immunodeficiency virus type I enhancer binding protein 3
207826_s_at	*ID3*	1·34	8·64	0·60	0·66	Inhibitor of DNA binding 3, dominant negative helix-loop-hetix protein
204549_at	*IKBKE*	2·33	1·29	0·71	0·66	Inhibitor of kappa light polypeptide gene enhancer in B cells
219878_s_at	*KLF13*	1·89	1·26	0·34	0·74	Kruppel-like factor 13
207667_s_at	*MAP2K3*	1·33	1·28	0·72	0·57	Mitogen-activated protein kinase kinase 3
201502_s_at	*NFKBIA*	2·31	1·29	0·71	0·57	Nuclear factor of κ light polypeptide gene enhancer in B cells inhibitor
222105_s_at	*NKIRAS2*	1·84	1·21	0·69	0·79	NFKB inhibitor interacting Ras-like 2
204622_x_at	*NR4A2*	1·35	4·31	0·65	0·63	Nuclear receptor subfamily 4, group A, member 2
207978_s_at	*NR4A3*	1·33	3·53	0·62	0·67	Nuclear receptor subfamily 4, group A, member 3
202600_s_at	*NRIPI*	1·86	1·39	0·26	0·61	Nuclear receptor interacting protein 1
216841_s_at	*SOD2*	1·25	1·73	0·36	0·75	Superoxide dismutase 2, mitochondrial
201416_at	*SOX4*	1·53	2·21	0·47	0·38	SRY (sex determining region Y)-box 4
223635_s_at	*SSBP3*	2·12	1·25	0·75	0·62	Single-stranded DNA binding protein 3
206506_s_at	*SUPT3H*	1·47	1·31	0·57	0·69	Suppressor of Ty 3 homologue (*S. cerevisiae*)
221618_s_at	*TAF9L*	1·25	1·49	0·47	0·75	TAF9-like RNA polymerase II
203177_x_at	*TFAM*	1·63	1·23	0·77	0·57	Transcription factor A, mitochondrial
213943_at	*TWIST1*	1·89	3·14	0·04	0·11	Twist homologue 1 (acrocephalosyndactyly 3; Saethre-Chotzen syndrome)
219836_at	*ZBED2*	1·33	4·76	0·67	0·21	Zinc finger, BED-type containing 2
211965_at	*ZFP36L1*	2·02	1·47	0·29	0·53	Zinc finger protein 36, C3H type-like 1
230760_at	*ZFY*	1·41	1·25	0·75	0·02	Zinc finger protein, Y-linked
228854_at	*ZNF145*	3·26	1·21	0·40	0·79	Transcribed locus
235121_at	*ZNF542*	2·68	1·33	0·63	0·67	Zinc finger protein 542

To investigate whether increased expression of the *IL-17* gene is a general feature of PB-derived $CD4^+$ T cells, we also tested *IL-17* gene expression in the above-described additional samples by real-time RT-PCR analysis. As shown in Fig. 6, all of four PB-derived $CD4^+$ T-cell samples revealed significantly increased gene expression of *IL-17* when compared with the CB-derived samples at 1 week. At 2 weeks, however, *IL-17* gene expression in PB-derived $CD4^+$ T cells was diminished while some of the CB-derived $CD4^+$ T cells (such as sample CB 4) exhibited increased *IL-17* gene expression. When the data were analysed statistically, expression of the *IL-17* gene was found to be

Table 4. Genes up-regulated in $CD4^+$ T cells from peripheral blood (PB)

Affi ID	Gene abbreviation	Fold change CB 1	CB 2	PB 1	PB 2	Gene name
Apoptosis						
1553681_a_at	*PRF1*	0·66	0·51	1·41	1·34	Perforin 1 (pore-forming protein)
B- and T-cell development						
224499_s_at	*AICDA*	0·06	0·44	1·56	3·47	Activation-induced cytidine deaminase
205495_s_at	*GNLY*	0·40	0·51	1·49	6·34	Granulysin
217478_s_at	*HLA-DMA*	0·67	0·39	1·33	1·35	Major histocompatibility complex, class II, DM alpha
203932_at	*HLA-DMB*	0·64	0·31	2·02	1·36	Major histocompatibility complex, class II, DM beta
211991_s_at	*HLA-DPA1*	0·50	0·14	1·54	1·50	Major histocompatibility complex, class II, DP alpha 1
212671_s_at	*HLA-DQA1*	0·44	0·23	1·56	2·56	Major histocompatibility complex, class II, DQ alpha 1
211656_x_at	*HLA-DQB1*	0·63	0·48	1·37	7·07	Major histocompatibility complex, class II, DQ beta 1
210982_s_at	*HLA-DRA*	0·58	0·37	1·50	1·42	Major histocompatibility complex, class II, DR alpha
208306_x_at	*HLA-DRB1*	0·51	0·24	1·49	1·61	Major histocompatibility complex, class II, DR beta 3
204670_x_at	*HLA-DRB5*	0·63	0·22	1·47	1·37	Major histocompatibility complex, class II, DR beta 5
211634_x_at	*IGHV1-69*	0·69	0·77	1·23	1·99	Immunoglobulin heavy variable 1–69
211645_x_at	*IgK*	0·15	0·49	1·51	6·62	Immunoglobulin kappa light chain (IGKV)
221651_x_at	*IGKC*	0·46	0·68	1·32	5·57	Immunoglobulin kappa constant
215379_x_at	*IGLC2*	0·62	0·41	1·38	4·26	Immunoglobulin lambda joining 2
209031_at	*IGSF4*	0·50	0·03	2·33	1·50	Immunoglobulin superfamily, member 4
205686_s_at	*CD86*	0·70	0·23	1·30	1·39	CD86 antigen (CD28 antigen ligand 2, B7-2 antigen)
204698_at	*ISG20*	0·68	0·49	1·32	1·64	Interferon stimulated exonuclease gene, 20 kDa
213915_at	*NKG7*	0·72	0·42	1·28	2·31	Natural killer cell group 7 sequence
Cell growth and maintenance						
201334_s_at	*ARHGEF12*	0·74	0·50	1·26	1·96	Rho guanine nucleotide exchange factor (GEF) 12
230292_at	*CHC1L*	0·70	0·56	1·30	2·02	Regulator of chromosome condensation (RCC1)
205081_at	*CRIP1*	0·56	0·73	1·27	1·75	Cysteine-rich protein 1 (intestinal)
31874_at	*GAS2L1*	0·77	0·52	1·23	2·35	Growth arrest-specific 2 like 1
202364_at	*MXI1*	0·43	0·73	1·27	1·44	MAX interactor 1
219304_s_at	*PDGFD*	0·65	0·71	1·29	3·68	Platelet-derived growth factor D
213397_x_at	*RNASE4*	0·64	0·46	1·36	2·21	Ribonuclease, RNase A family, 4
213566_at	*RNASE6*	0·69	0·39	1·49	1·31	Ribonuclease, RNase A family, k6
219077_s_at	*WWOX*	0·40	0·78	1·25	1·22	WW domain containing oxidoreductase
Cytokine and chemokine						
207861_at	*CCL22*	0·76	0·52	1·24	2·47	Chemokine (C–C motif) ligand 22
238750_at	*CCL28*	0·74	0·45	1·26	1·41	Chemokine (C–C motif) ligand 28
1555759_a_at	*CCL5*	0·71	0·23	1·29	1·92	Chemokine (C–C motif) ligand 5
208304_at	*CCR3*	0·50	0·12	1·50	2·35	Chemokine (C–C motif) receptor 3
205898_at	*CX3CR1*	0·30	0·20	1·70	4·16	Chemokine (C–X3–C motif) receptor 1
204533_at	*CXCL10*	0·80	0·16	1·20	2·53	Chemokine (C–X–C motif) ligand 10
219255_x_at	*IL-17RB*	0·73	0·04	1·27	1·29	Interleukin 17 receptor B
206148_at	*IL-3RA*	0·60	0·54	2·46	1·40	Interleukin 3 receptor, alpha (low affnity)
226333_at	*IL-6R*	0·22	0·79	1·21	2·43	Interleukin-6 receptor
206693_at	*IL-7*	0·09	0·54	1·46	5·86	Interleukin-7
Signal transduction						
204497_at	*ADCY9*	0·76	0·40	1·24	2·40	Adenylate cyclase 9
206170_at	*ADRB2*	0·58	0·35	1·42	3·97	Adrenergic, beta-2-, receptor, surface
202096_s_at	*BZRP*	0·50	0·54	1·59	1·46	Benzodiazapine receptor (peripheral)
230464_at	*EDG8*	0·04	0·09	1·91	2·42	Endothelial differentiation, sphingolipid G-protein-coupled receptor 8
223423_at	*GPR160*	0·54	0·68	1·40	1·32	G protein-coupled receptor 160
227769_at	*GPR27*	0·07	0·08	1·92	244	G protein in-coupled receptor 27
210095_s_at	*IGFBP3*	0·27	0·20	1·73	5·25	Insulin-like growth factor binding protein 3
38671_at	*PLXND1*	0·08	0·65	1·35	2·57	Plexin D1
226101_at	*PRKCE*	0·56	0·43	1·72	1·44	Protein kinase C. epsilon
232629_at	*PROK2*	0·01	0·13	1·87	2·09	Prokineticin 2

Table 4. Continued

Affi ID	Gene abbreviation	Fold change CB 1	CB 2	PB 1	PB 2	Gene name
203329_at	*PTPRM*	0·36	0·62	1·38	1·93	Protein tyrosine phosphatase, receptor type, M
204731_at	*TGFBR3*	0·78	0·55	1·22	2·04	Transforming growth factor, beta receptor III (betaglycan, 300 kDa)
Transcription						
203129_s_at	*KIF5C*	0·67	0·09	1·33	3·43	Kinesin family member 5C
213906_at	*MYBL1*	0·75	0·51	1·25	3·63	V-myb myeloblastosis viral oncogene homologue (avian)-like 1
209815_at	*PTCH*	0·59	0·27	1·41	4·17	Patched homologue (*Drosophila*)
213891_s_at	*TCF4*	0·74	0·65	2·06	1·26	Transcription factor 4
238520_at	*TRERFI*	0·70	0·77	1·23	2·30	Transcriptional regulating factor 1
203603_s_at	*ZFHX1B*	0·74	0·61	1·26	3·63	Zinc finger homobox 1b
213218_at	*ZNF187*	0·74	0·69	1·26	1·76	Zinc finger protein 187
221123_x_at	*ZNF395*	0·38	0·71	1·63	1·29	Zinc finger protein 395

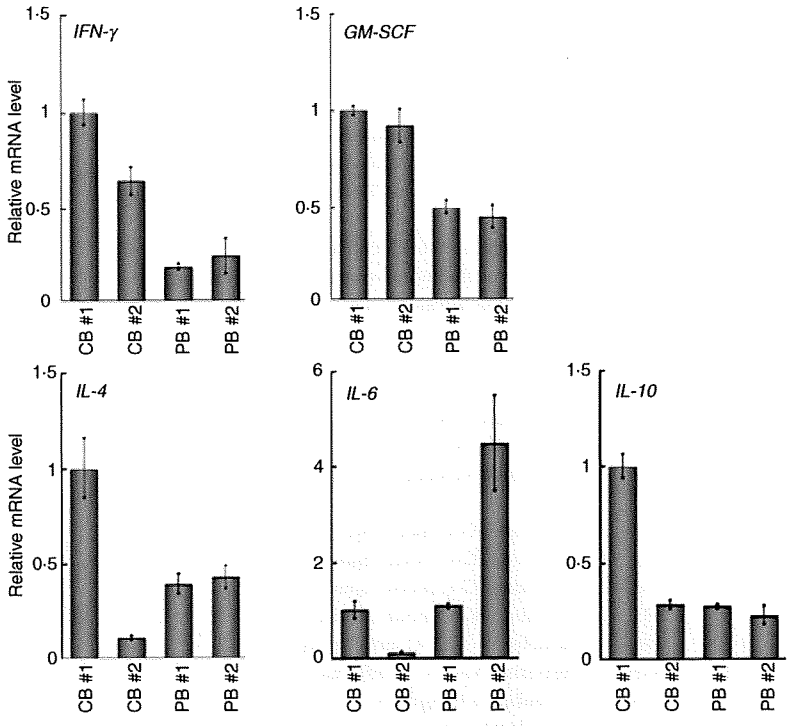

Figure 2. Quantitative polymerase chain reaction (PCR) analysis of the genes related to the T helper type 1 (Th1) and Th2 phenotypes. The expression of the genes indicated was examined by real-time reverse transcriptase (RT)-PCR using the same sample specimens as in Fig 1. Data are normalized to the mRNA level in PB 1 which is arbitrarily set to 1. The signal intensity was normalized using that of a control housekeeping gene [the human glyceraldehyde-3-phosphate dehydrogenase (*GAPDH*) gene]. Data are relative values with the standard deviation (SD) for triplicate wells.

significantly higher in PB-derived $CD4^+$ T cells in comparison with equivalent CB-derived $CD4^+$ T cells at 1 week ($P < 0·05$) but not at 2 weeks (Fig. 6).

Discussion

Although it is generally believed that there are functional differences between CB and PB lymphocytes, the details are obscure. For instance, Azuma *et al.*[13] reported that the phenotype and function of expanded CB lymphocytes were essentially equivalent to those of expanded PB lymphocytes when evaluated in *in vitro* experiments. In the present study, however, we have shown that CB-derived $CD4^+$ T cells revealed a distinct expression profile of genes important for the function of particular T-cell subsets compared with PB-derived $CD4^+$ T cells.

$CD4^+$ T cells can be classified into distinct subsets, including effector $CD4^+$ cells and Tregs, according to their functional characteristics as well as differentiation profiles.[14–16] Typically, effector $CD4^+$ T cells have been further divided into two distinct lineages on the basis of their cytokine production profiles, namely Th1 and Th2. Th1 cells producing cytokines such as IL-2, IFN-γ and GM-CSF have evolved to enhance the eradication of intracellular pathogens and are thought to be potent activators of cell-mediated immunity. In contrast, Th2

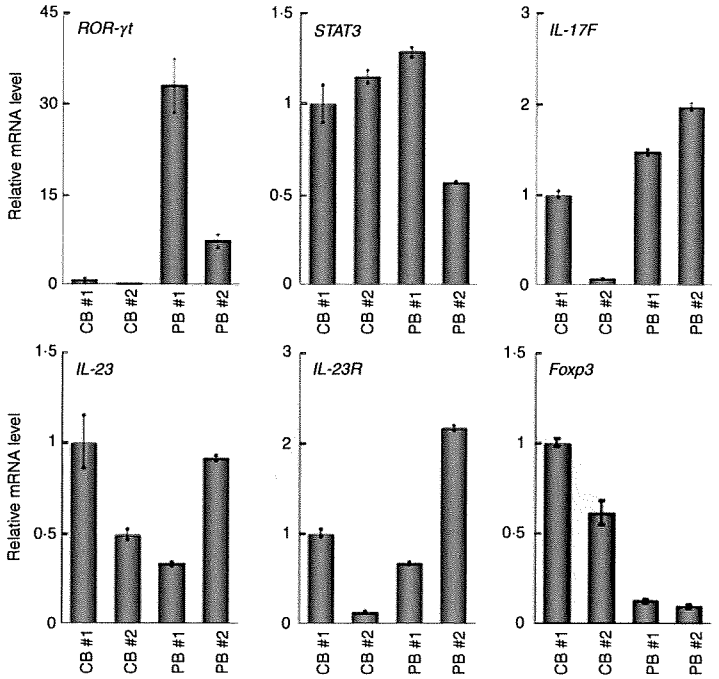

Figure 3. Quantitative polymerase chain reaction (PCR) analysis of the forkhead box protein 3 gene (*FOXP3*) and the genes related to the secretion of interleukin (IL)-17. The expression of the genes indicated was examined as in Fig 2. Data are normalized to the mRNA level in peripheral blood sample 1 (PB 1) as in Fig.2. The signal intensity was normalized using that of a control housekeeping gene [the human glyceraldehyde-3-phosphate dehydrogenase (*GAPDH*) gene]. Data are relative values with the standard deviation for triplicate wells.

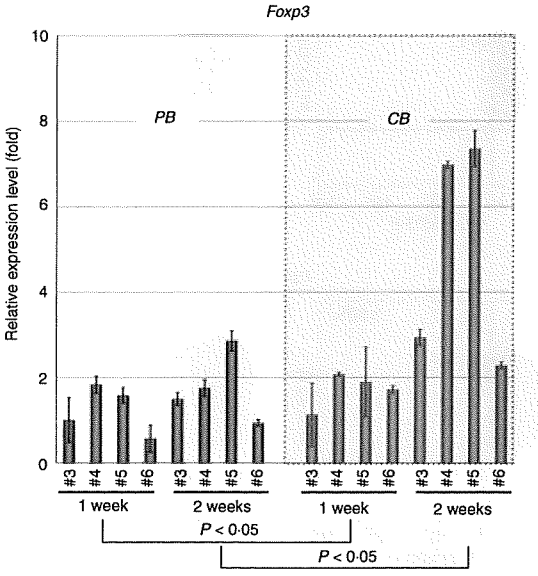

Figure 4. Quantitative polymerase chain reaction (PCR) analysis of the forkhead box protein 3 gene (*FOXP3*) in additional samples. Additional peripheral blood (PB) and cord blood (CB) samples were prepared and RNAs were extracted at 1 and 2 weeks. The expression of the *FOXP3* gene was examined as in Fig. 2. Data are normalized to the mRNA level in the sample of PB 3 at 1 week, which is arbitrarily set to 1. The signal intensity was normalized using that of a control housekeeping gene (the human β-actin gene). Data are relative values with the standard deviation for triplicate wells. The data were analysed statistically and *FOXP3* gene expression in CB-derived $CD4^+$ T cells was found to be significantly higher in comparison with equivalent PB-derived $CD4^+$ T cells at both 1 week ($P < 0{\cdot}05$) and 2 weeks ($P < 0{\cdot}05$).

cells secreting cytokines such as IL-4, IL-5, IL-6, IL-9 and IL-13 have evolved to enhance the elimination of parasitic infections and are thought to be potent activators of B-cell immunoglobulin E production, eosinophil recruitment, and mucosal expulsion. Th1-type responses to self or commensal floral antigens can promote tissue destruction and chronic inflammation, whereas dysregulated Th2-type responses can cause allergy and asthma. The development of Th1 is specified by the transcription factor T-bet (also known as Tbx-21) and master regulators of Th2 differentiation are GATA-3 and c-maf.

As shown in Fig. 2 and Table 2, the gene expression profiles of CB- and PB-derived $CD4^+$ T cells revealed no significant differences regarding cytokines related to the definition of Th1 and Th2, with the exceptions of IFN-γ and GM-CSF. The mRNA levels of IFN-γ and GM-CSF tended to be higher in CB-derived $CD4^+$ T cells than in PB-derived $CD4^+$ T cells. The mRNA expression of the transcription factors T-bet, GATA-3 and c-maf, which regulate Th1 and Th2 cell differentiation, did not differ significantly between CB- and PB-derived $CD4^+$ T cells.

In addition to Th1 and Th2 cells, IL-17 (also known as IL-17A)-producing T lymphocytes have been recently shown to comprise a distinct third subset of T helper cells, termed Th17 cells, in the mouse immune system. Th17 cells exhibit pro-inflammatory characteristics and act as major contributors to autoimmune disease. A number of experiments using animal models support a significant role for IL-17 in the response to allografts.[14,16,17] There is as yet no direct evidence for the existence of discrete Th17 cells in humans, although

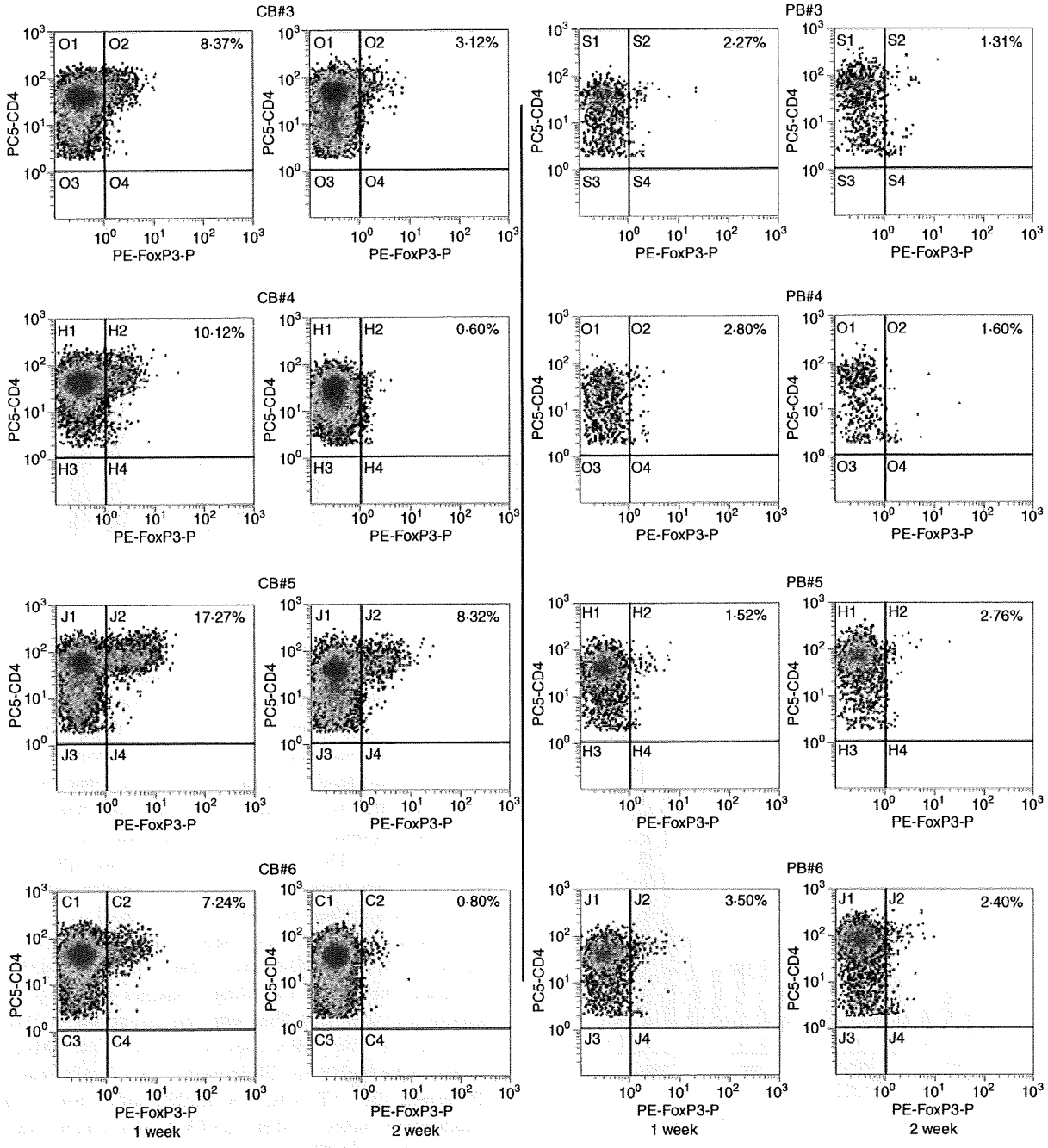

Figure 5. Protein expression of forkhead box protein 3 (Foxp3) in activated $CD4^+$ T cells. The protein expression of Foxp3 in same sample specimens as in Fig. 4 was examined by flow cytometry. The CD4 versus Foxp3 cytogram of the population gated with $CD3^+$ and $CD4^+$ in each sample is presented.

helper T cells secreting IL-17 have clearly been detected in the human immune system.[18] Several studies have shown a correlation between allograft rejection and IL-17. For example, IL-17 levels are elevated in human renal allografts during subclinical rejection and there are detectable mRNA levels in the urinary mononuclear cell sediments of these patients.[19,20] In human lung organ transplantation, IL-17 levels have also been reported to be elevated during acute rejection.[21] Interestingly, in this study, most of the PB-derived $CD4^+$ T-cell samples expressed higher levels of IL-17 mRNA than the CB-derived $CD4^+$ T-cell samples, suggesting that PB-derived $CD4^+$ T cells frequently include potent IL-17-secreting T cells.

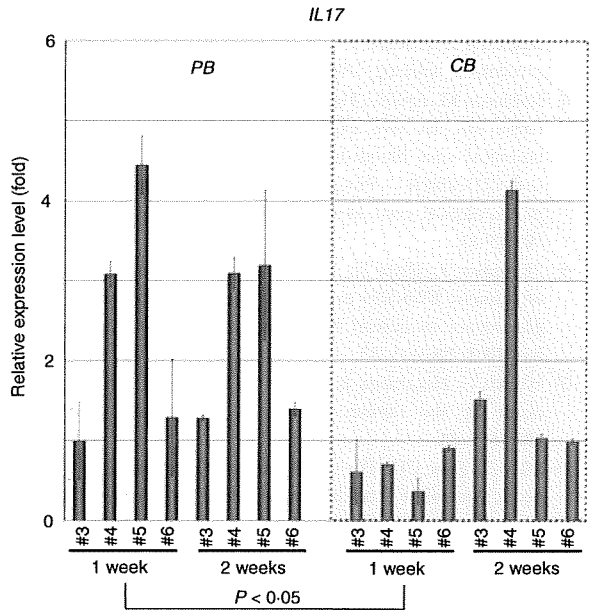

Figure 6. Quantitative polymerase chain reaction (PCR) analysis of interleukin (IL)-17 in additional samples. The expression of the *IL-17* gene in the same sample specimens as in Fig. 4 was examined and presented as in Fig 2. The data were analysed statistically and *IL-17* gene expression in peripheral blood (PB)-derived $CD4^+$ T cells was found to be significantly higher in comparison with equivalent CB-derived $CD4^+$ T cells at 1 week ($P < 0{\cdot}05$) but not at 2 weeks.

Th17 cells expand independently of T-bet or STAT-1. Ivanov *et al.*[22] have shown that the orphan nuclear receptor RORγt is the key transcription factor orchestrating the differentiation of the effector lineage. RORγt induces transcription of the gene encoding IL-17 in naïve $CD4^+$ T helper cells and is required for its expression in response to IL-6 and transforming growth factor (TGF)-β, the cytokines known to induce IL-17 expression. IL-23 is also involved in Th17 cell differentiation, but naïve T cells do not have the IL-23 receptor and are relatively refractory to IL-23 stimulation.[23,24] Although IL-23 seems to be an essential survival factor for Th17 cells, it is not required during their differentiation. It has been suggested that IL-23R expression is up-regulated on RORγt$^+$ Th17 cells in an IL-6-dependent manner. IL-23 may therefore function subsequent to IL-6/TGF-β-induced commitment to the Th17 lineage to promote cell survival and expansion and, potentially, the continued expression of IL-17 and other cytokines that characterize the Th17 phenotype. As presented in Fig. 3, the expression of the *RORγt* gene was significantly weaker in CB-derived $CD4^+$ T cells, whereas the expression of genes encoding IL-23 and the IL-23 receptor did not differ significantly between the $CD4^+$ T cells. Based on the above findings of others, it is possible that the low-level expression of the *RORγt* gene in CB-derived $CD4^+$ T cells is responsible for the absence of *IL-17* mRNA expression in those cells.

Tregs are another functional subset of T cells having anti-inflammatory properties and can cause quiescence of autoimmune diseases and prolongation of transplant function. *In vitro*, Tregs have the ability to inhibit the proliferation and production of cytokines by responder ($CD4^+$ $CD25^-$ and $CD8^+$) T cells subjected to polyclonal stimuli, as well as to down-regulate the responses of $CD8^+$ T cells, NK cells and $CD4^+$ cells to specific antigens.[25,26] These predicates translate *in vivo* to a great number of functions other than the maintenance of tolerance to self-components (prevention of autoimmune disease), such as the ability to prevent transplant rejection. Indeed, donor-specific Tregs can prevent allograft rejection in some models of murine transplant tolerance through a predominant effect on indirect alloresponses.

Foxp3 is thought to be responsible for the development of the Treg population and can act as a phenotypic marker of this fraction.[27] Tregs constitutively express CTLA-4 and there are suggestions that signalling through this pathway may be important for their function, as antibodies to CTLA-4 can inhibit Treg-mediated suppression.[28] As shown above, most of the CB-derived $CD4^+$ T cells were found to express either the *FOXP3* gene or the Foxp3 protein at higher levels compared with PB-derived $CD4^+$ T cells, suggesting that CB-derived $CD4^+$ T cells frequently include a potent Treg population.

As described above, *IL-17* mRNA was more detectable in PB-derived $CD4^+$ cells while *FOXP3* mRNA expression was higher in CB-derived $CD4^+$ cells. Post-transcriptional regulation, as well as differences in mRNA and protein turnover rates, can cause discrepancies between mRNA and protein expression and thus the differences observed in the mRNA expression do not necessary directly indicate those in protein expression.[29] Indeed, we observed some discrepancy between the levels of mRNA and protein with regard to Foxp3 expression in CB-derived $CD4^+$ T cells, as presented above. Nevertheless, changes in mRNA expression are mediated by the alteration of transcriptional regulation, and thus should indicate the differentiation ability of the cells. Therefore, our data indicate that CB-derived $CD4^+$ T cells tend frequently to include potent Tregs, while PB-derived $CD4^+$ T cells tend to include potent IL-17-secreting cells. As described above, DLI with donor CB-derived activated $CD4^+$ T cells is currently becoming established as a routine therapeutic strategy in Japan. It has been proposed that the skewing of responses towards Th17 or Th1 cells and away from Tregs may be responsible for the development and/or progression of autoimmune diseases or acute transplant rejection, and it may thus also be speculated that CB-derived $CD4^+$ T cells are more appropriate for DLI than PB-derived $CD4^+$ T cells.

However, our data also indicate the presence of individual, donor-dependent variations in the characteristics of activated $CD4^+$ T cells derived from CB and PB. More-

over, activated $CD4^+$ T cells do not consist of a single population and should include several distinct functional subsets of $CD4^+$ T cells. Therefore, it is important to clarify the characteristics of activated $CD4^+$ T cells in each preparation to predict the therapeutic effect of DLI in each clinical case.

In summary, our findings demonstrate a difference in gene expression between activated $CD4^+$ T cells derived from CB and those derived from PB. The higher level of *FOXP3* gene expression and the lower level of *IL-17* gene expression in CB-derived $CD4^+$ T cells may indicate that these cells have potential as immunomodulators in DLI therapy. Further detailed analysis should reveal the advantages of activated $CD4^+$ T cells from CB in DLI.

Acknowledgements

We thank the Tokyo Cord Blood Bank for the distribution of cord blood for research use. This work was supported by a grant from the Japan Health Sciences Foundation for Research on Publicly Essential Drugs and Medical Devices (KHC2032), Health and Labour Sciences Research Grants (the 3rd term comprehensive 10-year strategy for cancer control H19-010, Research on Children and Families H18-005, Research on Human Genome Tailor-made and Research on Publicly Essential Drugs and Medical Devices H18-005), and a Grant for Child Health and Development from the Ministry of Health, Labour and Welfare of Japan. It was also supported by CREST, JST.

Disclosures

No competing personal or financial interests exist for any of the authors in relation to this manuscript.

References

1 Loren AW, Porter DL. Donor leukocyte infusions after unrelated donor hematopoietic stem cell transplantation. *Curr Opin Oncol* 2006; **18**:107–14.
2 Roush KS, Hillyer CD. Donor lymphocyte infusion therapy. *Transfus Med Rev* 2002; **16**:161–76.
3 Alyea EP, Soiffer RJ, Canning C *et al.* Toxicity and efficacy of defined doses of CD4(+) donor lymphocytes for treatment of relapse after allogeneic bone marrow transplant. *Blood* 1998; **91**:3671–80.
4 Giralt S, Hester J, Huh Y *et al.* CD8-depleted donor lymphocyte infusion as treatment for relapsed chronic myelogenous leukemia after allogeneic bone marrow transplantation. *Blood* 1995; **86**:4337–43.
5 Tomizawa D, Aoki Y, Nagasawa M *et al.* Novel adopted immunotherapy for mixed chimerism after unrelated cord blood transplantation in Omenn syndrome. *Eur J Haematol* 2005; **75**:441–4.
6 Cohena Y, Nagler A. Hematopoietic stem-cell transplantation using umbilical-cord blood. *Leuk Lymphoma* 2003; **44**:1287–99.
7 Parmar S, Robinson SN, Komanduri K *et al.* Ex vivo expanded umbilical cord blood T cells maintain naive phenotype and TCR diversity. *Cytotherapy* 2006; **8**:149–57.
8 Robinson KL, Ayello J, Hughes R, van de Ven C, Issitt L, Kurtzberg J, Cairo MS. Ex vivo expansion, maturation, and activation of umbilical cord blood-derived T lymphocytes with IL-2, IL-12, anti-CD3, and IL-7. Potential for adoptive cellular immunotherapy post-umbilical cord blood transplantation. *Exp Hematol* 2002; **30**:245–51.
9 Miyagawa Y, Okita H, Nakaijima H *et al.* Inducible expression of chimeric EWS/ETS proteins confers Ewing's family tumor-like phenotypes to human mesenchymal progenitor cells. *Mol Cell Biol* 2008; **28**:2125–37.
10 Werlen G, Hausmann B, Naeher D, Palmer E. Signaling life and death in the thymus: timing is everything. *Science* 2003; **299**:1859–63.
11 Riley JL, June CH. The CD28 family: a T-cell rheostat for therapeutic control of T-cell activation. *Blood* 2005; **105**:13–21.
12 Woo EY, Yeh H, Chu CS, Schlienger K, Carroll RG, Riley JL, Kaiser LR, June CH. Cutting edge: regulatory T cells from lung cancer patients directly inhibit autologous T cell proliferation. *J Immunol* 2002; **168**:4272–6.
13 Azuma H, Yamada Y, Shibuya-Fujiwara N *et al.* Functional evaluation of ex vivo expanded cord blood lymphocytes: possible use for adoptive cellular immunotherapy. *Exp Hematol* 2002; **30**:346–51.
14 Afzali B, Lombardi G, Lechler RI, Lord GM. The role of T helper 17 (Th17) and regulatory T cells (Treg) in human organ transplantation and autoimmune disease. *Clin Exp Immunol* 2007; **148**:32–46.
15 Castellino F, Germain RN. Cooperation between CD4+ and CD8+ T cells: when, where, and how. *Annu Rev Immunol* 2006; **24**:519–40.
16 Reiner SL. Development in motion: helper T cells at work. *Cell* 2007; **129**:33–6.
17 Bi Y, Liu G, Yang R. Th17 cell induction and immune regulatory effects. *J Cell Physiol* 2007; **211**:273–8.
18 Fossiez F, Djossou O, Chomarat P *et al.* T cell interleukin-17 induces stromal cells to produce proinflammatory and hematopoietic cytokines. *J Exp Med* 1996; **183**:2593–603.
19 Loong CC, Hsieh HG, Lui WY, Chen A, Lin CY. Evidence for the early involvement of interleukin 17 in human and experimental renal allograft rejection. *J Pathol* 2002; **197**:322–32.
20 Van Kooten C, Boonstra JG, Paape ME *et al.* Interleukin-17 activates human renal epithelial cells in vitro and is expressed during renal allograft rejection. *J Am Soc Nephrol* 1998; **9**:1526–34.
21 Vanaudenaerde BM, Dupont LJ, Wuyts WA *et al.* The role of interleukin-17 during acute rejection after lung transplantation. *Eur Respir J* 2006; **27**:779–87.
22 Ivanov II, McKenzie BS, Zhou L, Tadokoro CE, Lepelley A, Lafaille JJ, Cua DJ, Littman DR. The orphan nuclear receptor RORgammat directs the differentiation program of proinflammatory IL-17+ T helper cells. *Cell* 2006; **126**:1121–33.
23 Langrish CL, Chen Y, Blumenschein WM *et al.* IL-23 drives a pathogenic T cell population that induces autoimmune inflammation. *J Exp Med* 2005; **201**:233–40.
24 Oppmann B, Lesley R, Blom B *et al.* Novel p19 protein engages IL-12p40 to form a cytokine, IL-23, with biological activities similar as well as distinct from IL-12. *Immunity* 2000; **13**: 715–25.

25 Dieckmann D, Plottner H, Berchtold S, Berger T, Schuler G. Ex vivo isolation and characterization of CD4(+) CD25(+) T cells with regulatory properties from human blood. *J Exp Med* 2001; **193**:1303–10.

26 Wing K, Lindgren S, Kollberg G, Lundgren A, Harris RA, Rudin A, Lundin S, Suri-Payer E. CD4 T cell activation by myelin oligodendrocyte glycoprotein is suppressed by adult but not cord blood CD25+ T cells. *Eur J Immunol* 2003; **33**:579–87.

27 Wan YY, Flavell RA. Identifying Foxp3-expressing suppressor T cells with a bicistronic reporter. *Pro Natl Acad Sci USA* 2005; **102**:5126–31.

28 Read S, Greenwald R, Izcue A, Robinson N, Mandelbrot D, Francisco L, Sharpe AH, Powrie F. Blockade of CTLA-4 on CD4+ CD25+ regulatory T cells abrogates their function in vivo. *J Immunol* 2006; **177**:4376–83.

29 Hack CJ. Integrated transcriptome and proteome data: the challenges ahead. *Brief Funct Genomic Proteomic* 2004; **3**:212–9.

Identification of Severe Combined Immunodeficiency by T-Cell Receptor Excision Circles Quantification Using Neonatal Guthrie Cards

Yoichi Morinishi, MD, PhD, Kohsuke Imai, MD, PhD, Noriko Nakagawa, MD, Hiroki Sato, MHSc, Katsuyuki Horiuchi, MD, PhD, Yoshitoshi Ohtsuka, MD, PhD, Yumi Kaneda, MD, Takashi Taga, MD, PhD, Hiroaki Hisakawa, MD, PhD, Ryosuke Miyaji, MD, Mikiya Endo, MD, Tsutomu Oh–ishi, MD, PhD, Yoshiro Kamachi, MD, PhD, Koshi Akahane, MD, Chie Kobayashi, MD, PhD, Masahiro Tsuchida, MD, PhD, Tomohiro Morio, MD, PhD, Yoji Sasahara, MD, PhD, Satoru Kumaki, MD, PhD, Keiko Ishigaki, MD, PhD, Makoto Yoshida, MD, PhD, Tomonari Urabe, MD, Norimoto Kobayashi, MD, PhD, Yuri Okimoto, MD, PhD, Janine Reichenbach, MD, PhD, Yoshiko Hashii, MD, PhD, Yoichiro Tsuji, MD, PhD, Kazuhiro Kogawa, MD, PhD, Seiji Yamaguchi, MD, PhD, Hirokazu Kanegane, MD, PhD, Toshio Miyawaki, MD, PhD, Masafumi Yamada, MD, PhD, Tadashi Ariga, MD, PhD, and Shigeaki Nonoyama, MD, PhD

Objective To assess the feasibility of T-cell receptor excision circles (TRECs) quantification for neonatal mass screening of severe combined immunodeficiency (SCID).

Study design Real-time PCR based quantification of TRECs for 471 healthy control patients and 18 patients with SCID with various genetic abnormalities (*IL2RG*, *JAK3*, *ADA*, *LIG4*, *RAG1*) were performed, including patients with maternal T-cell engraftment (n = 4) and leaky T cells (n = 3).

Results TRECs were detectable in all normal neonatal Guthrie cards (n = 326) at the levels of 10^4 to 10^5 copies/μg DNA. In contrast, TRECs were extremely low in all neonatal Guthrie cards (n = 15) and peripheral blood (n = 14) from patients with SCID, including those with maternal T-cell engraftment or leaky T cells with hypomorphic RAG1 mutations or LIG4 deficiency. There were no false-positive or negative results in this study.

Conclusion TRECs quantification can be used as a neonatal mass screening for patients with SCID. *(J Pediatr 2009;155:829-33).*

See related article, p 834

Severe combined immunodeficiency (SCID) is a genetic disorder characterized by the absence of T-cells and adaptive immunity.[1,2] Affected infants usually have severe infections due to opportunistic pathogens in the first months of life. Hematopoietic stem cell transplantation can reconstitute immune function, although severe infections before hematopoietic stem cell transplantation can be fatal to the patients within the first year of life.[3,4] Thus, early diagnosis before the occurrence of severe infection is essential.[5-7]

Four different mechanisms have been identified as a cause of SCID, including purine metabolism defects, defective signaling of the common γ-chain–dependent cytokine receptors, defective V(D)J recombination, and defective pre-TCR/TCR signaling.[1,2] Although human SCID is caused by mutations of at least 10 different genes, all patients have a characteristic decreased number of newly

BCG	Bacillus Calmette-Guérin
BMT	Bone marrow transplantation
CMV	Cytomegalovirus
FISH	Fluorescent in situ hybridization
HSCT	Hematopoietic stem cell transplantation
PB	Peripheral blood
PCR	Polymerase chain reaction
sjTRECs	Signal joint TRECs
SCID	Severe combined immunodeficiency
TCR	T-cell receptor
TRECs	T-cell receptor excision circles
UCB	Umbilical cord blood

From the Department of Pediatrics (Y.M., K.I., N.N., K.H., Y.T., K.K., S.N.), National Defense Medical College, Saitama, Japan; the Department of Medical Informatics (K.I., H.S.), National Defense Medical College Hospital, Saitama, Japan; the Department of Pediatrics (Y.O., Y.K.), Hyogo College of Medicine, Hyogo, Japan; Department of Pediatrics (T.T.), Shiga University of Medical Science, Shiga, Japan; the Department of Pediatrics (H.H.), Kochi University, Kochi, Japan; the Department of Pediatrics (R.M.), University of Occupational and Environmental Health, Fukuoka, Japan; the Department of Pediatrics (M.E.), Iwate Medical University, Iwate, Japan; the Division of Infectious Diseases, Immunology, and Allergy (T.O.), Saitama Children's Medical Center, Saitama, Japan; the Department of Pediatrics (Y.K.), Nagoya University Graduate School of Medicine, Aichi, Japan; the Department of Pediatrics (K.A.), Yamanashi Prefectural Central Hospital, Yamanashi, Japan; the Department of Pediatrics (C.K., M.T.), Ibaraki Children's Hospital, Ibaraki, Japan; the Department of Pediatrics (T.M.), Tokyo Medical and Dental University, Tokyo, Japan; the Department of Pediatrics (Y.S., S.K.), Tohoku University, Miyagi, Japan; the Department of Pediatrics (K.I.), Tokyo Women's Medical University, Tokyo, Japan; the Department of Pediatrics (M.Y.), Asahikawa Medical College, Hokkaido, Japan; the Department of Pediatrics (T.U.), Kumamoto University, Kumamoto, Japan; the Department of Interdisciplinary Medicine (N.K.), Nagano Children's Hospital, Nagano, Japan; the Department of Hematology/Oncology (Y.O.), Chiba Children's Hospital, Chiba, Japan; the Department of Immunology/Hematology/BMT (J.R.), University Children's Hospital Zurich, Zurich, Switzerland; the Department of Pediatrics (Y.H.), Osaka University, Osaka, Japan; the Department of Pediatrics (S.Y.), Shimane University, Shimane, Japan; the Department of Pediatrics (H.K., T.M.), University of Toyama, Toyama, Japan; and the Department of Pediatrics (M.Y., T.A.), Hokkaido University, Hokkaido, Japan

Supported by grants from the Ministry of Defense, Ministry of Health, Labour and Welfare Kawano Masanori Foundation for Promotion of Pediatrics, Jeffrey Modell Foundation, and The Mother and Child Health Foundation. The authors declare no conflicts of interest.

 10.1016/j.jpeds.2009.05.026

Table. Genotype, lymphocyte subset, and TRECs of patients with SCID

Patient	Sex	Genotype	Age at onset of symptoms	Age at SCID diagnosis	Lymphocytes (/μL)	CD3+ (%)	CD3+ (/μL)	CD19+ (%)	CD45RO+ / CD4 + CD3 + (%)	Maternal lymphocyte engraftment	Guthrie cards TRECs (/μg DNA)	PB Pre-HSCT TRECs (/μg DNA)	PB Pre-HSCT Age
1	M	*IL2RG*	3 mo	3 mo	720	0.0	0	-	86.0	-	<10	-	-
2	M	*IL2RG*	-	0 mo	780	0.0	0	-	94.0	-	<10	<10	0 y, 0 mo
3	M	*IL2RG*	-	0 mo	920	0.0	0	-	91.0	-	<10	<10	0 y, 0 mo
4	M	*IL2RG*	4 mo	5 mo	2550	0.2	5	NA	99.4	-	<10	<10	0 y, 5 mo
5	M	*IL2RG*	10 mo	10 mo	1035	0.0	0	-	94.7	-	<10	<10	0 y, 10 mo
6	M	*IL2RG*	4 mo	5 mo	3560	0.0	0	-	95.8	-	<10	<10	0 y, 5 mo
7	M	*IL2RG*	-	0 mo	966	0.7	7	95.3	77.5	-	<10	<10	0 y, 0 mo
8	M	*JAK3*	4 mo	4 mo	3810	0.0	0	-	87.0	-	<10	-	-
9	F	*JAK3*	2 mo	5 mo	2495	0.0	0	-	89.8	-	<10	<10	0 y, 6 mo
10	M	*ADA*	1 mo	4 mo	90	40.0	36	99.5	4.4	-	<10	<10	0 y, 2 mo
11	M	*ADA*	1 mo	2 m	100	6.8	7	89.9	0.9	-	6.2×10^2	<10	0 y, 1 mo
12	M	*IL2RG*	8 mo	8 mo	3250	40.8	1326	89.8	65.5	T + NK+	-	<10	1 y
13	M	*IL2RG*	-	0 mo	950	4.2	40	NA	68.6	T+	<10	-	-
14	M	*IL2RG*	9 mo	10 mo	860	7.0	60	99.6	85.9	T + NK+	<10	<10	0 y, 10 mo
15	M	*IL2RG*	3 mo	3 mo	300	36.5	110	NA	53.5	T+	<10	-	-
16	F	*LIG4*	-	0 mo	550	38.7	213	97.6	0.3	-	-	<10	2 y
17	M	*LIG4*	1 y, 6 mo	4 y	300	44.3	133	25.2	0.1	-	<10	<10	4 y
18	F	*RAG1*	8 mo	1 y 9 mo	550	53.1	292	91.6	12.0	-	-	8.0×10^1	2 y

NA, Not available.

developed T cells.[1,2,8,9] T-cell receptor excision circles (TRECs) are small circular DNA fragments formed through rearrangement of the T-cell receptor (TCR) α locus and do not multiply during cell division.[9-13] Therefore, TRECs quantification is reportedly useful for determining recent thymic emigrants. Two reports of a method for neonatal screening of SCID using TRECs quantification by real-time PCR have been published.[6,7] Both studies quantified TRECs of patients with SCID using peripheral blood and found significantly lower levels of TRECs than those of control neonates. In addition, Guthrie cards from 2 patients with SCID retrospectively had undetectable TRECs.[6] Most control neonates had high amounts of TRECs. However, TRECs were undetectable in some samples. To increase specificity, 1 study[7] proposed a 2-tiered strategy using a combination of quantified TRECs and IL-7.

We have evaluated blood from Guthrie cards and peripheral blood from control patients and patients with SCID for detecting TRECs.

Methods

Peripheral blood samples were obtained from 112 healthy volunteers (median age, 14 years; range, 0.1 to 51 years). Thirty-three umbilical cord blood samples (median gestational age, 38.9 weeks) were collected at the National Defense Medical College Hospital. Dried blood spots of umbilical cord blood were obtained by applying 50 μL of residual blood to the 11-mm circles on filter-paper cards (PKU-S, Toyoroshi, Tokyo, Japan). Twenty-six neonatal Guthrie cards with dried blood spots were donated from surplus routine samples for newborn mass screening from neonates born at National Defense Medical College Hospital during this study period (January 2005 to December 2007). In addition, 300 neonatal Guthrie cards, stored at −20°C for less than 5 years in a neonatal mass screening center at Shimane University, were analyzed.

Eighteen patients with SCID were analyzed for TRECs (Table). All patients were genetically diagnosed using genomic DNA sequencing. Mutations of either *IL2RG* (n = 11), *JAK3* (n = 2), *RAG1* (n = 1), *ADA* (n = 2), or *LIG4* (n = 2) were identified in the patients (Table).

Peripheral blood samples of 14 patients before hematopoietic stem cell transplantation were used. In addition, neonatal Guthrie cards of 15 patients that had been stored in newborn mass screening centers were obtained.

Maternal T and NK lymphocyte engraftment was diagnosed by fluorescent in situ hybridization (FISH) using X and Y chromosome–specific probes after purification of each compartment by specific monoclonal antibodies and immunomagnetic beads.

The study protocol was approved by the National Defense Medical College Institutional Review Board, and informed consent was obtained from the parents of patients with SCID and healthy control patients, as well as adult control patients, in accordance with the Declaration of Helsinki.

Quantification of TRECs by Real-Time PCR

We used 100 μL of whole blood (EDTA anticoagulated peripheral blood and heparinized cord blood) or 2 punches of 6 mm in diameter from Guthrie card to extract genomic DNA.

Concentrations of DNA from peripheral blood, fresh dried blood punches from normal neonates (n = 26), and stored dried blood spots from normal neonates (n = 300) were

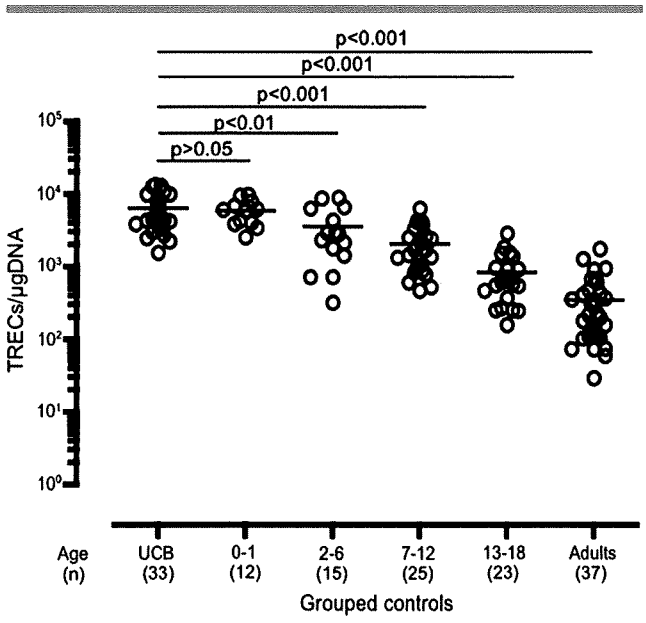

Figure 1. Umbilical cord blood (UCB) (n = 33) and peripheral blood (n = 112, 0 to 51 years) samples were analyzed. TRECs in different age groups are shown. TRECs were significantly higher in umbilical cord blood ($6.2 \pm 3.2 \times 10^3$ copies/μg DNA) and infants ($5.8 \pm 2.3 \times 10^3$ copies/μg DNA) as compared with other age groups of children ($3.5 \pm 2.8 \times 10^3$ copies/μg DNA in 2 to 6 years old, $2.0 \pm 1.4 \times 10^3$ copies/μg DNA in 7 to 12 years old, $8.2 \pm 6.3 \times 10^2$ copies/μg DNA in 13 to 18 years old) and adults ($3.4 \pm 3.6 \times 10^2$ copies/μg DNA).

40.6 ± 2.3 ng/μL (mean $\pm$ SEM) (range, 13 to 167 ng/μL), 7.8 ± 2.8 ng/μL (2.9 to 13.0 ng/μL), and 5.3 ± 0.2 ng/μL (0.6 to 20.2 ng/μL), respectively.

Quantitative real-time PCR for δRec-$\psi J\alpha$ sjTRECs was performed using the same primers and δRec probes as reported by Hazenberg et al.[14]

As an internal control, RNaseP gene was amplified in each sample tested using TaqMan RNaseP Primer-Probe (VIC dye) Mix (Applied Biosystems, Foster City, California).

Statistical Analysis

An exponential regression model was used to quantify the relationship between age and TRECs levels (per μg DNA and per RNaseP). Goodness-of-fit of the model was evaluated by R^2. The Dunnett multiple comparison test was conducted to test the differences of each age group (0 to 1, 2 to 6, 7 to 12, 13 to 18 years and adults) versus umbilical cord blood comparisons serving as a control group (Figure 1). RNaseP and TRECs levels of patients with SCID and control patients were compared by an unpaired Student t test (if the variance was equal) or Welch t test (if the variance was different).

All statistical analyses were performed using GraphPad Prism Version 4.00 (GraphPad Software, San Diego, California). $P < .05$ denotes a statistically significant difference.

Results

TRECs were detectable in all DNA samples from whole blood of normal control patients, including umbilical cord blood (n = 33), healthy infants (0 to 1 year old, n = 12), children (2 to 18 years old, n = 63), and adults (n = 37). TRECs in whole blood were found to decline with increasing age ($r = 0.851$). TRECs of umbilical cord blood were significantly higher than those of children and adults but were not significantly different from those of infants (Figure 1). We found a strong correlation between TRECs copies/μg DNA and TRECs/RNaseP ratio ($r = 0.979$).

TRECs of peripheral blood samples from all 14 patients with SCID before hematopoietic stem cell transplantation were below detectable levels (<10 copies/μg DNA) with the exception of 1 (P18, see below), in contrast to high levels of control infants ($5.8 \pm 0.7 \times 10^3$/μg DNA, n = 12) ($P < .0001$) (Figure 2, A).

Next, we analyzed TRECs of dried blood spots from normal control neonates using simulated Guthrie cards from cord blood (n = 31), neonatal Guthrie cards obtained during this study period (January 2005 to December 2007) (n = 26), and those stored in a neonatal mass screening center for less than 5 years (n = 300). TRECs were detectable in all dried blood spots: in cord blood ($1.3 \pm 0.1 \times 10^4$ copies/μg DNA, mean $\pm$ SEM), in neonatal Guthrie cards ($2.3 \pm 0.2 \times 10^4$ copies/μg DNA), and in stored neonatal Guthrie cards ($3.6 \pm 0.2 \times 10^5$ copies/μg DNA).

To determine whether this method can identify patients with SCID, we quantified TRECs using 15 stored neonatal Guthrie cards from patients with SCID (patients 1 through 11, 13 through 15, and patient 17). RNaseP levels were high in all neonatal Guthrie cards from patients with SCID ($1.8 \pm 0.3 \times 10^6$ copies/μg DNA, n = 15), which were similar to control levels ($2.3 \pm 0.1 \times 10^6$ copies/μg DNA, n = 26) ($P = .184$), indicating an appropriate amount of genomic DNA was extracted from the neonatal Guthrie cards (Figure 2, B). In contrast, TRECs were below detection levels in all patients ($P < .0001$) except 1 (patient 11). This patient with SCID had compound heterozygous mutations of *ADA* (Gln119Stop/Arg34Ser). He had detectable but significantly lower levels of TRECs (6.2×10^2 copies/μg DNA) than those of control neonates ($2.3 \pm 0.2 \times 10^4$ copies/μg DNA, n = 26) (Figure 2, B). At 1 month of age, the TRECs from the peripheral blood of patient 11 were below detectable levels (Table and Figure 2, A).

These results indicate that neonatal mass screening of SCID by quantitative real-time PCR for TRECs using neonatal Guthrie cards is feasible.

We analyzed TRECs in 4 patients with SCID with maternal T-cell engraftment (patients 12 through 15, $CD3^+$ cells: 40 to 1326/μL). We found that all patients had undetectable levels of TRECs in neonatal Guthrie cards (patients 13 through 15) and peripheral blood (patients 12 and 14). Patient 12 had a normal lymphocyte count (3250/μL) on admission as well as a significant number of T, B, and NK cells (Table). His peripheral blood TRECs level was below the detection

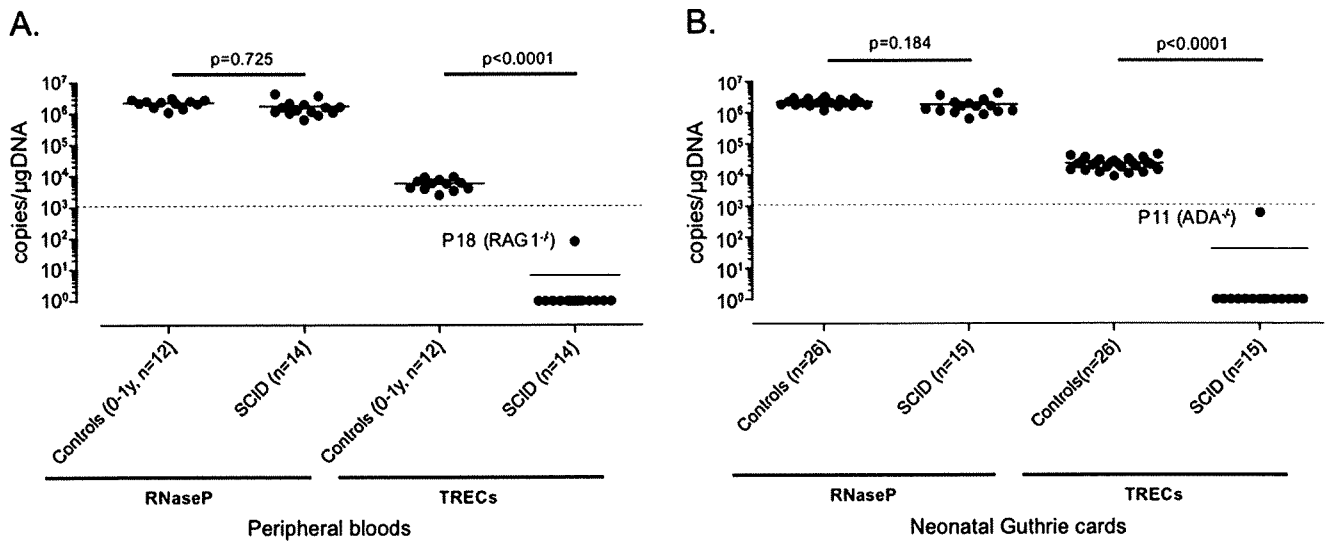

Figure 2. A, RNaseP levels in peripheral blood from patients with SCID ($2.1 \pm 0.2 \times 10^6$ copies/μg DNA, n = 14) were comparable with those from control infants ($2.2 \pm 0.2 \times 10^6$ copies/μg DNA, n = 12) ($P = .725$). Peripheral blood TRECs from all typical patients with SCID were undetectable (<10 copies/μg DNA) as compared with the high copy number of peripheral blood TRECs from control neonates ($5.8 \pm 0.7 \times 10^3$ copies/μg DNA, n = 12) ($P < .0001$). Patient 18, with hypomorphic RAG1 mutations, had detectable but extremely low TRECs in peripheral blood (8.0×10^1 copies/μg DNA). **B,** RNaseP levels in neonatal Guthrie cards from patients with SCID ($1.8 \pm 0.3 \times 10^6$ copies/μg DNA, n = 15) were comparable with those from control neonates ($2.3 \pm 0.1 \times 10^6$ copies/μg DNA, n = 26) ($P = .184$). TRECs of Guthrie cards from 14 of 15 patients with SCID during the early neonatal period were undetectable (<10 copies/μg DNA). An ADA-deficient patient ($ADA^{-/-}$, patient 11) had detectable but significantly low TRECs levels (6.2×10^2 copies/μg DNA) compared with control neonates ($2.3 \pm 0.2 \times 10^4$ copies/μg DNA, n = 26).

levels despite the presence of peripheral T cells. FISH analysis revealed that all circulating $CD3^+$ cells (1326/μL) were derived from his mother. Similarly, TRECs of other patients (patients 13 through 15) were also undetectable despite the maternal T cells (Table).

These results confirm the findings of Patel et al[9] indicating that TRECs quantification is both effective and reliable for the screening of SCID even in the presence of maternal T cells.

Patient 18 with hypomorphic *RAG1* mutations was lymphopenic (550/μL) at 21 months of age, but T (53.1%), B (12.0%), and NK cells (31.2%) were present in peripheral blood. Both T cells with TCR$\alpha\beta$ chain and TCR$\gamma\delta$ chain were derived from the patient, as determined by FISH analysis of the sex chromosome.

The peripheral blood TRECs from this patient (8.0×10^1 copies/μg DNA) (Figure 2, A) was significantly lower than age-matched control patients ($5.2 \pm 3.2 \times 10^3$ copies/μg DNA, n = 5). We purified T cells with TCR$\alpha\beta$ chain by FACS sorting. T cells with TCR$\alpha\beta$ from patient 18 had very low TRECs/cells (4.0×10^1 copies/10^5 cells) than those of age-matched control patients (5.1×10^3 copies/10^5 cells).

We also analyzed TRECs in 2 LIG4-deficient patients (patients 16 and 17) who had leaky T cells (Table). Peripheral blood TRECs were undetectable in both patients (Figure 2, A), and TRECs in the neonatal Guthrie card were also undetectable in patient 17 (Figure 2, B).

These results indicate that TRECs are extremely low in patients with SCID, even if leaky T cells are present.

Discussion

We demonstrated that TRECs were undetectable, or were significantly lower (10^1 to 10^2 copies/μg DNA) than healthy neonates and infants (10^4 to 10^5 copies/μg DNA), in both neonatal Guthrie cards and peripheral blood samples obtained from SCID. All types of SCID tested, including IL2RG, JAK3, ADA, RAG1, LIG4 deficiencies, were identified by measuring TRECs. This finding was consistent with the previous reports that showed the usefulness of TRECs for the identification of SCID[6,7,9] and further indicates that TRECs can identify SCID with maternal T cells and SCID with leaky T cells. In 2 LIG4-deficient patients with leaky T cells (CD3 + 38.7% and 44.3%) and in 1 patient with hypomorphic mutations in *RAG1* gene, who had immunodeficiency and autoimmunity with residual memory T cells,[15,16] TRECs were undetectable. These results indicate that TRECs is a good marker to identify the defect of V(D)J recombination, in which LIG4 and RAG1 play essential roles. We observed progressive loss of TRECs in a patient with SCID and ADA deficiency (patient 11). This observation is compatible with the report that the loss of naive T lymphocytes occurs after birth in patients with ADA deficiency.[17,18]

No false-negative was observed in this study (TRECs were below normal range in all cases of SCID), although sample size was too small to determine the exact false-negative rate.

Consistently, there were no false-positive (TRECs were all positive) in the control samples in this study. The previous studies showed 2.9% and 7.7% of false-positive rates.[6,7] The primers and probe used in this study [14] were different from previously studies.[6,7] However, both probes were found to result in equivalent quantities (data not shown). Thus, the reason of the different false-positive rate between this and the previous studies is currently undetermined. Mass screening using larger population will disclose the exact false-positive and false-negative rate.

The cost to test 1 sample in our study is $5 per sample, which was reported to be cost-effective.[19] We are now trying to further reduce the cost.

Early diagnosis of SCID can prevent severe and recurrent infection, which is often fatal and makes stem cell transplantation difficult. Identification of SCID by newborn screening by TRECs will improve the prognosis and quality of life of patients with SCID. ■

We thank the patients and their families who participated in this study. We also thank Mrs Makiko Tanaka for her skillful technical assistance and members of Department of Obstetrics and Gynecology, National Defense Medical College for collecting umbilical cord blood samples.

Submitted for publication Oct 10, 2008; last revision received April 22, 2009; accepted May 19, 2009.

Reprint requests: Dr Kohsuke Imai, National Defense Medical College, 3-2 Namiki, Tokorozawa, Saitama, Japan, 359-8513. E-mail: kimai@ndmc.ac.jp.

References

1. Fischer A, Le Deist F, Hacein-Bey-Abina S, Andre-Schmutz I, BasileGde S, de Villartay JP, et al. Severe combined immunodeficiency: a model disease for molecular immunology and therapy. Immunol Rev 2005;203:98-109.
2. Buckley RH. Molecular defects in human severe combined immunodeficiency and approaches to immune reconstitution. Annu Rev Immunol 2004;22:625-55.
3. Buckley RH, Schiff SE, Schiff RI, Markert L, Williams LW, Roberts JL, et al. Hematopoietic stem-cell transplantation for the treatment of severe combined immunodeficiency. N Engl J Med 1999;340:508-16.
4. Antoine C, Muller S, Cant A, Cavazzana-Calvo M, Veys P, Vossen J, et al. Long-term survival and transplantation of haemopoietic stem cells for immunodeficiencies: report of the European experience 1968-99. Lancet 2003;361:553-60.
5. Myers LA, Patel DD, Puck JM, Buckley RH. Hematopoietic stem cell transplantation for severe combined immunodeficiency in the neonatal period leads to superior thymic output and improved survival. Blood 2002;99:872-8.
6. Chan K, Puck JM. Development of population-based newborn screening for severe combined immunodeficiency. J Allergy Clin Immunol 2005; 115:391-8.
7. McGhee SA, Stiehm ER, Cowan M, Krogstad P, McCabe ER. Two-tiered universal newborn screening strategy for severe combined immunodeficiency. Mol Genet Metab 2005;86:427-30.
8. Buckley RH, Schiff RI, Schiff SE, Markert ML, Williams LW, Harville TO, et al. Human severe combined immunodeficiency: genetic, phenotypic, and functional diversity in one hundred eight infants. J Pediatr 1997;130:378-87.
9. Patel DD, Gooding ME, Parrott RE, Curtis KM, Haynes BF, Buckley RH. Thymic function after hematopoietic stem-cell transplantation for the treatment of severe combined immunodeficiency. N Engl J Med 2000; 342:1325-32.
10. de Villartay JP, Hockett RD, Coran D, Korsmeyer SJ, Cohen DI. Deletion of the human T-cell receptor delta-gene by a site-specific recombination. Nature 1988;335:170-4.
11. Douek DC, McFarland RD, Keiser PH, Gage EA, Massey JM, Haynes BF, et al. Changes in thymic function with age and during the treatment of HIV infection. Nature 1998;396:690-5.
12. McFarland RD, Douek DC, Koup RA, Picker LJ. Identification of a human recent thymic emigrant phenotype. Proc Natl Acad Sci U S A 2000;97:4215-20.
13. Hazenberg MD, Verschuren MC, Hamann D, Miedema F, van Dongen JJ. T cell receptor excision circles as markers for recent thymic emigrants: basic aspects, technical approach, and guidelines for interpretation. J Mol Med 2001;79:631-40.
14. Hazenberg MD, Otto SA, CohenStuart JW, Verschuren MC, Borleffs JC, Boucher CA, et al. Increased cell division but not thymic dysfunction rapidly affects the T-cell receptor excision circle content of the naive T cell population in HIV-1 infection. Nat Med 2000;6: 1036-42.
15. de Villartay JP, Lim A, Al-Mousa H, Dupont S, Dechanet-Merville J, Coumau-Gatbois E, et al. A novel immunodeficiency associated with hypomorphic RAG1 mutations and CMV infection. J Clin Invest 2005;115: 3291-9.
16. Ehl S, Schwarz K, Enders A, Duffner U, Pannicke U, Kuhr J, et al. A variant of SCID with specific immune responses and predominance of gamma delta T cells. J Clin Invest 2005;115:3140-8.
17. Giblett ER, Anderson JE, Cohen F, Pollara B, Meuwissen HJ. Adenosine-deaminase deficiency in two patients with severely impaired cellular immunity. Lancet 1972;2:1067-9.
18. Hershfield MS. Genotype is an important determinant of phenotype in adenosine deaminase deficiency. Curr Opin Immunol 2003;15:571-7.
19. McGhee SA, Stiehm ER, McCabe ER. Potential costs and benefits of newborn screening for severe combined immunodeficiency. J Pediatr 2005; 147:603-8.

Int J Hematol (2009) 90:455–462
DOI 10.1007/s12185-009-0408-0

ORIGINAL ARTICLE

Phenotypic variations between affected siblings with ataxia-telangiectasia: ataxia-telangiectasia in Japan

Tomohiro Morio · Naomi Takahashi · Fumiaki Watanabe · Fumiko Honda · Masaki Sato · Masatoshi Takagi · Ken-ichi Imadome · Toshio Miyawaki · Domenico Delia · Kotoka Nakamura · Richard A. Gatti · Shuki Mizutani

Received: 26 May 2009 / Revised: 31 July 2009 / Accepted: 3 August 2009 / Published online: 25 August 2009

Abstract A nationwide survey was conducted for identifying ataxia-telangiectasia (AT) patients in Japan. Eighty-nine patients were diagnosed between 1971 and 2006. Detailed clinical and laboratory data of 64 patients including affected siblings were collected. Analyses focused on malignancy, therapy-related toxicity, infection, and hematological/immunological parameters. The phenotypic variability of AT was assessed by comparing 26 affected siblings from 13 families. Malignancy developed in 22% of the cases and was associated with a high rate of severe therapy-related complications: chemotherapy-related cardiac toxicity in 2 children, and severe hemorrhagic cystitis requiring surgery in 2 patients. The frequency of serious viral infections correlated with the T cell count. Hypogammaglobulinemia with hyper-IgM (HIGM) was recorded in 5 patients, and 3 patients developed pan-hypogammaglobulinemia. Differences in immunological parameters were noted in siblings. Four patients showed an HIGM phenotype, in contrast to their siblings with normal IgG and IgM levels. The patients with HIGM phenotype showed reduced levels of TRECs and $CD27^{+}CD20^{+}$ memory B cells. The findings suggest that hitherto unidentified modifier genes or exogenous environmental factors can influence the overall immune responses. Our data along with future prospective study will lead to better understanding of the hematological/immunological phenotypes and to better care of the patients.

Keywords Ataxia-telangiectasia · Phenotypic variations · Hyper-IgM · Modifier genes · Affected siblings

T. Morio (✉) · N. Takahashi · F. Watanabe · F. Honda · M. Sato · M. Takagi · S. Mizutani
Department of Pediatrics and Developmental Biology, Tokyo Medical and Dental University Graduate School of Medical and Dental Sciences, 1-5-45 Yushima, Bunkyo-ku, Tokyo 113-8519, Japan
e-mail: tmorio.ped@tmd.ac.jp

K. Imadome
Department of Infectious Diseases, National Research Institute for Child Health and Development, Tokyo, Japan

T. Miyawaki
Department of Pediatrics, Toyama University School of Medicine, Toyama, Japan

D. Delia
Department of Experimental Oncology, Istituto Nazionale Tumori, Milan, Italy

K. Nakamura · R. A. Gatti
Department of Pathology and Laboratory Medicine, David Geffen School of Medicine, University of California, Los Angeles, CA, USA

1 Introduction

This is the first survey with regard to ataxia-telangiectasia (AT) carried out in Japan.

AT is a rare genetic disorder having multiple manifestations. It is characterized by early-onset of progressive neurodegeneration, oculocutaneous telangiectasia, various immunodeficiencies leading to a predisposition to infection, high risk of developing lymphoreticular malignancy, and increased sensitivity to ionizing radiation. Characteristic laboratory and diagnostic findings include cerebellar atrophy, high serum alpha-fetoprotein (AFP) level, and chromosomal translocations involving immunoglobulin and T cell receptor genes [1–5].

Clinical heterogeneity is observed within the disorder [1, 3, 5–8]. Neurological symptoms include cerebellar ataxia, oculomotor apraxia, disarthria, and choreoathetosis,

which range from classical form with steady progression to milder forms with milder phenotype or slower progression.

Predisposition to infection because of impaired immunity is noted; however, it is variable [1, 4, 6]. Lower respiratory infections increase with age, partly as a consequence of food aspiration caused by deterioration of neurological functions.

The immune defect is rarely progressive and is variable among AT patients [1, 8, 9]. The common humoral abnormalities are decreased levels of IgA, IgE, and IgG2. The most notable defect in T cell immunity is lymphopenia, especially in the CD4 T cell population; however, 30% of patients do not show immunodeficiency [8].

Following cloning of a gene responsible for AT, diagnosis of AT could be confirmed by measuring ATM protein, ATM kinase activity, or by sequencing the ataxia-telangiectasia mutated (*ATM*) gene [2, 10, 11]. ATM plays a controlling role in (1) recognition and repair of DNA damage by interaction with H2AX, Mre11/Rad50/NBS1, and SCM1; (2) cell cycle arrest by phosphorylation of various molecules, including Brca1, Chk2, and E2F1; and (3) cellular apoptosis via MDM2 and the p53 pathway [3, 12–14].

Despite progress in identification of the molecular basis of ATM function, little research evidence is available concerning the pathogenesis of AT or therapies that might aid the AT patients [15–18]. This reflects the relative rarity of this disorder, and thus the paucity of data from large patient cohorts. Particularly, the severe adverse effects of chemotherapeutic agents leading to increased DNA damage in AT patients with malignancies need further scrutiny.

This prompted us to conduct a nationwide survey in Japan with regard to AT, and to collect data on the clinical signs/symptoms, long-term follow-up laboratory data, and complications of treatment. Basic immunological studies were performed on patients currently alive. We reassessed the disease survival rate and compared the data from affected siblings to determine the phenotypic variability between patients with similar genotypes and environments. We describe here therapy-related toxicity, hematological/immunological changes, and phenotypic diversity in the affected siblings.

2 Methods

2.1 Patients and questionnaire

In September 2005, a preliminary questionnaire soliciting information about AT patients was sent to 1,223 departments of 665 medical hospitals/institutes in Japan. A more extensive questionnaire was conducted for 92 potential AT patients. Eighty-nine patients were enrolled in this analysis after elimination of non-AT patients and overlapping information; and detailed information was obtained from the remaining 64 patients. The data were provided after obtaining informed consent from the patients currently alive or their parents.

AT diagnosis of patients was conducted at their respective institutes and reconfirmed at our institute by assessing the clinical symptoms, laboratory findings, and carrying out genetic analysis, protein expression analysis, or both in some cases. The study included 28 sibling cases, of which 26 patients from 13 families were subjected to comparative analysis.

2.2 Western blotting

In order to prepare cellular extracts for anti-ATM immunoblotting, the T cells from the AT patients were expanded in the presence of recombinant IL-2 (700 IU/mL; Proleukin, Chiron, Amsterdam, Netherland) in a flask with immobilized anti-CD3 mAb:OKT3 (5 μg/mL, Janssen-Kyowa, Tokyo, Japan). Western blotting with anti-ATM antibody was performed as previously described [19, 20].

Mutational analysis was performed as described previously [21, 22] and will be reported in a separate paper. The analyses were approved by the ethics committee of our university, and written informed consent was obtained from the patients and/or their parents.

2.3 Immunological characterization

Surface immunophenotyping was performed as previously described [23–25]. Data for T cell-receptor excision circles (TRECs) were calculated using peripheral mononuclear cells as described previously [26]. The quality of the extracted DNA was confirmed by the measurement of GAPDH, and TRECs level was expressed as copy number/μgDNA.

2.4 Statistical analysis

The probability of survival was estimated by the product-limit method. Student's *t* test was applied for statistical analysis between the two groups.

3 Results

3.1 Diagnosis and survival

The median age at diagnosis was 6.7 years (range 0.9–24.5 years), and the median age of survival was 26.0 years (Fig. 1). Twenty-nine patients had died before the study began, at a median age of 19.7 years (range 5.8–31.8 years).

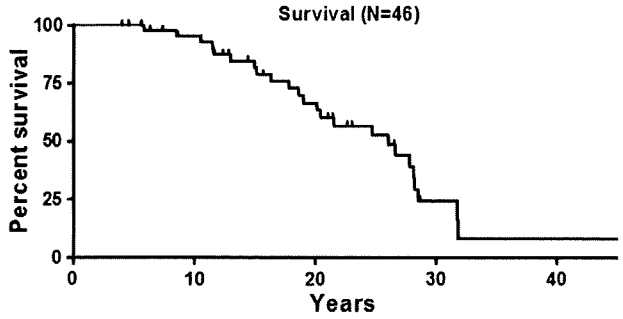

Fig. 1 Survival rates of 46 ataxia-telangiectasia (AT) patients. Survival rates of 46 patients as calculated by Kaplan–Meier method. The median survival was 26 years

The most frequently documented cause of death was infection (18 patients), and 5 of 18 patients died of infection during chemotherapy for malignancy. In the remaining 11 patients, 3 patients died of malignancy, 5 patients from various other causes, and 3 from unknown etiology.

The median age of the patients currently alive was 15.0 years (range 4–28.6 years). The median age of onset of telangiectasia was recorded as 6.7 years (range 1.8–13.5 years). Clinical characteristics of the patients are displayed in Table 1.

3.2 Neurological symptoms

Neurological symptoms are summarized in Table 1. Tremor, oculomotor apraxia, and chorea were observed in 68, 59, and 27% of the patients, respectively. Thirty of 45 patients were wheelchair-bound at the median age of 8.0 years (range 2.5–16.4 years).

3.3 Malignancies

Detailed information was obtained from 12 patients with malignancy. Of these patients, 6 had acute lymphoblastic leukemia (ALL; 4 T-ALL and 2 Precursor-B-ALL), 4 had non-Hodgkin lymphoma, 1 had Langerhans cell histiocytosis, and 1 developed cholangiocarcinoma. Two patients achieved long-term complete remission, 3 died of tumor progression, 4 died of bacterial infections during chemotherapy, and 1 died of cytomegalovirus (CMV) infection during the period of chemotherapy-related immunodeficiency. One patient died as a result of infection before starting therapy, and 1 patient died because of cardiac failure due to chemotherapy.

Altogether two patients with T-ALL suffered from the left cardiac failure caused by chemotherapy that included anthracycline. During maintenance therapy with methotrexate and 6-mercaptoprine, 1 patient with precursor-B-ALL developed inflammation of multiple lymph nodes with NK-cell cytosis which rapidly developed into multiple organ failure. Although the definitive diagnosis was not made, this was probably due to EBV-associated NK-cell lineage proliferative disorder.

Hemorrhagic cystitis requiring surgical intervention was noted in 2 patients. One patient with idiopathic thrombocytopenic purpura (ITP) refractory to gammaglobulin treatment and steroid therapy, received intravenous cyclophosphamide. Although the patient maintained a platelet level >50,000/mm^3, massive hemorrhage in the bladder developed 3 years after completing cyclophosphamide therapy. This patient also suffered from acute nephritis accompanied by acute renal failure before developing ITP [27]. The second patient received a cyclophosphamide-containing regimen for the treatment of ALL, and

Table 1 Patient characteristics

Male/female	40/40
Sibling cases/patients without a sibling	28/52
Maternal breast cancer	2.2% (1/46)
Age at diagnosis (age, years): median (range)	6.7 (0.9–24.5)
Alive/deceased	28/29
Median age of survival: median (range)	26.0 (5.8–31.8)
Onset of telangiectasia (age, years): median (range)	6.7 (1.8–13.5)
Neurological symptoms	
Onset of ataxia (age, years): median (range)	1.5 (0.5–5.6)
Ataxia	100% (80/80)
Apraxia	59% (26/44)
Chorea	27% (12/44)
Infections (number)	
Bacterial infection	29
Severe viral infection	11
Malignancy	22% (17/76)
Acute leukemia	6
Lymphoma	4
Langerhans cell histiocytosis	1
Cholangiocarcinoma	1
Unknown	5
Glucose intolerance	17% (8/46)
Growth retardation (height <2.0 SD at >6 years)	86% (19/22)
Hypothyroidism	0%
Other clinical symptoms	
Hemorrhagic cystitis (post-chemotherapy)	2
Cardiac failure (post-chemotherapy)	2
Acute nephritis/renal failure	1
Heart failure	1
Paroxysmal supraventricular tachycardia	1
ITP	1

Eighty-nine patients were enrolled in this analysis; and detailed information was obtained in 64 patients. Positive in the total numbers of the reply is indicated in parenthesis when % is calculated. Total number in each reply does not add up to 89 or to 64, since not all the question items were answered

developed massive hemorrhage during maintenance therapy with methotrexate and 6-mercaptopurine. Cytoscopy revealed varicose veins in the bladder of both of the patients.

3.4 Infections

Twenty-nine patients had bacterial infections mainly of the sinus or the lower respiratory tract. Eleven patients had severe or persistent viral infections, of which 3 suffered from chronic Epstein-Barr virus (EBV) infection, 2 from severe recurrent varicella-zoster virus (VZV) infection, 2 from severe measles pneumonia, 1 from herpes simplex virus (HSV) encephalitis, and 1 from systemic CMV infection after a treatment course for T-ALL. $CD3^+$T cell counts were known in 7 patients and were less than 450/mm^3 in 5 patients. T cell-lymphopenia did not result from chemotherapy for malignancy. One of the patients had EBV infection after completion of therapy for malignant lymphoma.

Anti-EBV titers were documented in 19 patients. Five had anti-EBV titers indicative of persistently active EBV infection: elevated VCA IgG (>1,280×) and EA-DR IgG (>40×). Of the 5 patients, 4 showed negative anti-EBNA antibody (<10×) and 1 had a normal EBNA response (40×).

None of the patients in this cohort had fungal infections caused by agents such as *Candida, Aspergillus,* or *Pneumocystis jerovicii*, or protozoal infections.

3.5 Hematological and immunological data

Serum AFP level was elevated in 43 of the 44 patients tested. The median serum concentration of AFP was 372 ng/mL (range 71–1,518).

Average neutrophil count, lymphocyte count, hemoglobin levels, and platelet levels were 5,620/mm^3, 1,610/mm^3, 13.0 g/dL, and 40.2 × 10^4/mm^3, respectively. Data on lymphocyte subsets were recorded in 29 patients. $CD3^+$T cell count was <1,000/mm^3 in 24 patients and was decreased (>2 SD below the mean for age) in 66% of patients. $CD4^+$T cells, $CD8^+$T cells, and $CD20^+$B cells were decreased in 76, 39, and 78% of patients, respectively. Distribution of each subset is shown in Fig. 2. The TRECs were measured in mononuclear cells of 12 patients, and were significantly lower than those in age-matched controls (Fig. 3) in concordance with previously reported data [9, 28]. There was no correlation between the $CD3^+$T cell counts and the TRECs levels (data not shown).

Five of ten patients with ≤450/mm^3 $CD3^+$lymphocytes, whereas 2 out of 19 patients with >450/mm^3 $CD3^+$T cells developed severe viral infection ($p < 0.05$).

Immunoglobulin levels were evaluated in 50 patients (Fig. 4). Four patients (8%) showed elevated IgM level

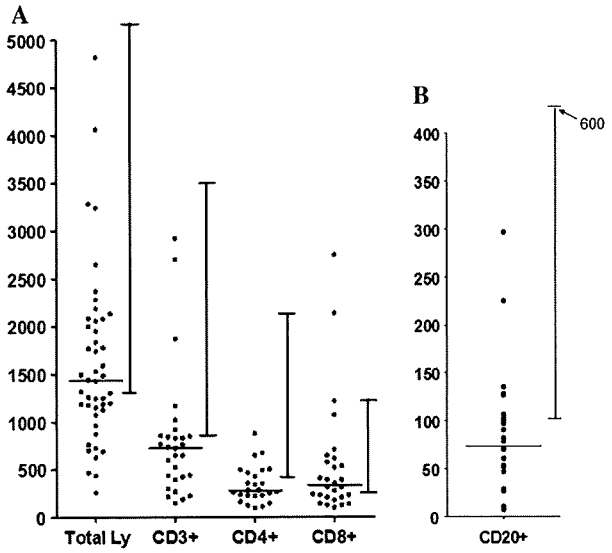

Fig. 2 Lymphocyte counts of patients with AT. Total lymphocytes, $CD3^+$, $CD4^+$, $CD8^+$ (**a**) and $CD20^+$ cell counts (**b**) are shown. *Horizontal bar* shows median value of the cell counts. Normal ranges (5th–95th percentiles) for patients aged 10 years to adults are shown on the *right side* of each column

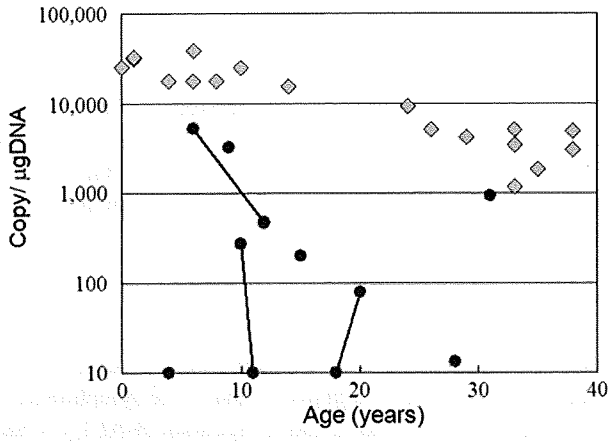

Fig. 3 Quantification of T cell receptor excision circles (TRECs) in AT patients. *Closed diamonds* show TRECs in normal healthy subjects. *Closed circles* are TRECs measured in AT patients. *Solid lines* connect data for affected siblings

(>450 mg/dL) with normal or elevated IgG level (1,050–2,513 mg/dL). Three patients showed normal IgA level, and 1 patient showed absence of IgA. Whether they had polyclonal or monoclonal gammopathy is not known. IgG level was <500 mg/dL in 8 patients. Reduced serum levels of IgG and IgM were recorded in 3 patients on more than 2 separate occasions. Two of the 3 patients developed hematological malignancy thereafter. Serum IgA level was below 50 mg/dL in 17 patients (34%), of which 10 patients had isolated IgA deficiency.

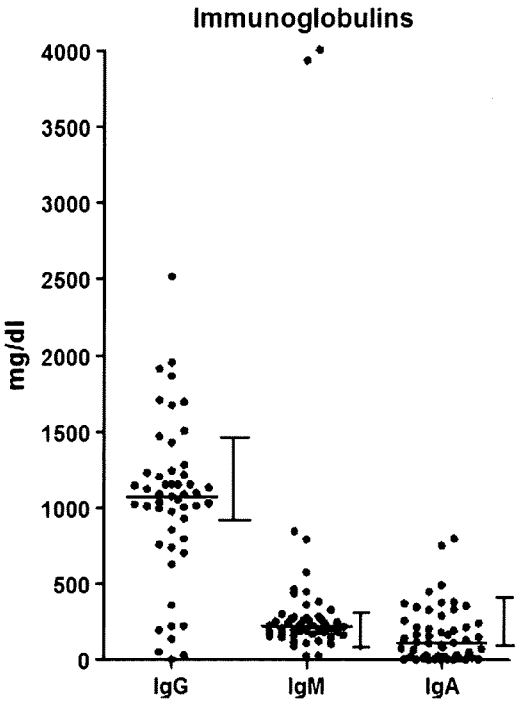

Fig. 4 Serum IgG, IgM, and IgA levels of AT patients. *Horizontal bar* shows median value. Normal ranges (5th–95th percentiles) for patients aged 10 years to adults are shown on the *right side* of each column

Decreased IgG levels (0–220 mg/dL) with hyper-IgM (380–4,000 mg/dL) (HIGM) were noted in 5 of 8 patients with low IgG. Lymphocyte subsets were examined in 3 patients with the HIGM phenotype (IgM: 790, 3,800, and 4,000 mg/dL). They showed decreased B cell counts (10, 52, and 82 cells/mm^3). The CD27$^+$CD20$^+$population, recorded in 2 out of 3 HIGM patients, showed decreased memory B cell fraction (<15% of CD20$^+$B cells). The TRECs level was particularly low, with <100 copies/μgDNA in both patients.

3.6 Comparison of phenotypes in affected siblings

Phenotypic description and laboratory data from 13 pairs of affected siblings were collected at comparable age whenever possible. Sequencing and Western blot analyses were performed in 6 families. ATM mutations were different in all families (manuscript in preparation), and ATM expression was virtually absent (<2% of normal ATM level) in all the cases. The results of anti-ATM Western blot for representative patients are shown in Fig. 5.

Some neurological and endocrinological findings were concordant in AT siblings. Chorea was noted in 5 patients. Two sibling pairs were concordant. In another family, only a younger brother showed chorea. Diabetes mellitus was detected in 5 siblings in 3 families.

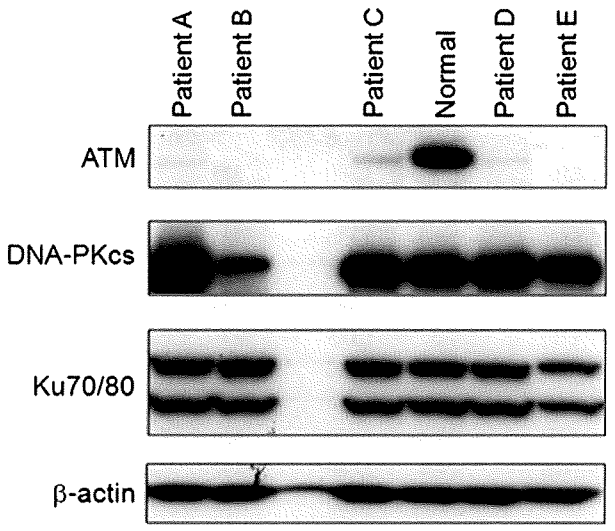

Fig. 5 Western blot analysis for ATM. Protein extracted from activated T cells from normal subjects and from clinically diagnosed AT patients (*Patient A, B, C, D,* and *E*) were subjected to Western blot analysis for ATM. The blots were also probed with antibodies to DNA-PKcs, Ku70/80, and to β-actin

Differences were noted in some associated symptoms and laboratory data (Table 2). Serum AFP level was more than three times higher in the elder sibling in 2 sibling pairs, higher in the younger sibling in 2 families, and almost at the same level in 6 sibling pairs. In 2 siblings, the elder brother had acute nephritis, ITP, hemorrhagic cystitis, and was obese, with an elevated serum triglyceride level (>400 mg/dL), whereas a younger brother was emaciated with a low triglyceride level (<30 mg/dL) with none of the disorders of his brother.

A large variation was noted in hematological and immunological parameters (Table 2). In 3 families, the lymphocyte count was consistently more than three times higher in one sibling than the other sibling (>2,000/mm^3). Decreased IgG/IgA with hyper-IgM was recorded in 4 patients. HIGM was detected before the age of 2 years in 3 patients, and was recorded at the age of 10 years in 1 patient, whereas it was not observed in their siblings: IgG/IgM/IgA levels were normal in 3 patients, and 1 patient showed only decreased IgA. Except for 3 patients with HIGM, 3 patients had low serum IgA levels, while the IgA levels of their siblings were normal or elevated.

No significant differences were observed in the CD3$^+$, CD4$^+$, CD8$^+$, or CD20$^+$ counts in the sibling pairs. TRECs were measured in 6 siblings from 3 families. Slight differences were observed in TRECs values; however, this could be because of the age difference.

Common features of AT patients with HIGM phenotype were low memory B cell count and low TRECs level. The CD27$^+$CD20$^+$memory B cell/CD27$^-$CD20$^-$naïve B cell ratio was 0.2/1.5% in 1 patient with HIGM, while that of